arXiv:hep-ph/0208123v3 26 Jan 2004

Systematics of quark-antiquark states and scalar exotic mesons

V.V. Anisovich

Abstract

The analysis of the experimental data of Crystal Barrel Collaboration on the $p\bar{p}$ annihilation in flight with the production of mesons in the final state resulted in a discovery of a large number of mesons over the region 1900–2400 MeV, thus allowing us to systematize quark-antiquark states in the (n, M^2) and (J, M^2) planes, where n and J are radial quantum number and spin of the meson with the mass M. The data point to meson trajectories in these planes being approximately linear, with a universal slope. The sector of scalar mesons is discussed in more detail, where, on the basis of the recent K-matrix analysis, the nonet classification of quark–antiquark states was performed: in the region below 2000 MeV, two scalar nonets are fixed, that is, the basic one and the nonet of the first radial excitation. In the scalar sector, there are two states with the isospin $I = 0$, which are extra ones with respect to the quark–antiquark classification, i.e. exotic states: the broad resonance $f_0(1200 - 1600)$ and the light σ-meson. The ratios of coupling constants for hadronic decays to the states $\pi\pi, K\bar{K}, \eta\eta, \eta\eta'$ point to the gluonium nature of the broad state $f_0(1200 - 1600)$.

Contents.

1. Introduction.
2. Experimental data of the Crystal Barrel Collaboration and systematics of mesons states.
2.1 Systematics of meson states.
2.2 Exotics: the states off quark–antiquark trajectories.
3. Scalar-meson sector.
3.1 The K-matrix analysis of the $(IJ^{PC} = 00^{++})$-wave.
3.1.1 K-matrix amplitude.
3.1.2 Partial amplitude for the 00^{++} wave: unitarity, analyticity and the problem of the left-hand cut.
3.1.3 Three-meson production in the reactions of the $p\bar{p}$ and $n\bar{p}$ annihilation.
3.1.4 Peripheral two-meson production in meson–nucleon collisions at high energies.
3.2 Classification of scalar bare states.
3.3 Overlapping f_0-resonances in the region 1200–1700 MeV: the accumulation of widths of quark-antiquark states by the glueball.
3.4 Evolution of couplings of the 00^{++}-states with channels $\pi\pi$, $\pi\pi\pi\pi$, $K\bar{K}$, $\eta\eta$ $\eta\eta'$ with the onset of the decay processes.
3.5 Evaluation of the glueball component in the resonances $f_0(980)$, $f_0(1300)$, $f_0(1500)$, $f_0(1750)$ and broad state $f_0(1200-1600)$ based on the analysis of hadronic channels.
3.6 The light σ-meson: Is there a pole of the 00^{++}-wave amplitude?
3.7 Systematics of scalar states on the (n, M^2) and (J, M^2) planes and the problem of basic multiplet $1^3P_0 q\bar{q}$.
3.7.1 The K-matrix classification of scalars and $q\bar{q}$ trajectories in the (n, M^2) planes.
3.7.2 Systematics of kaons in the (J, M^2) plane.
3.8 Exotic scalar states, $f_0(1200-1600)$ and $f_0(300-500)$.
4. Conclusion.

1 Introduction

To understand the structure of strong interactions at low and moderate energies is one of the highest-priority problems of the modern particle physics. In the last decades, great efforts have been paid to develop the strong-interaction theory, the strong QCD, with a considerable progress though without determinate breakthrough. One may believe that, in part, this was due to a poor knowledge, up to recent time, of the experimental situation in meson sector.

To enlighten experimental situation, a number of experiments had been undertaken during 1990–2000 directed purposefully to the search for new meson resonances, and a detailed investigation of mesons discovered before was carried out.

The Crystal Barrel Collaboration accumulated one of the richest statistics on the $p\bar{p}$ and $n\bar{p}$ annihilation reactions; the group of physicists from PNPI took part in the analysis and interpretation of the data by Crystal Barrel Collaboration (a brief review of this activity is given in [1]); this survey presents the results of recent investigations.

In 1993–1994, two groups, QMWC (London) and PNPI (St.Petersburg), were analysing meson spectra obtained in reactions of the $p\bar{p}$ annihilation at rest. As a result, the scalar-isoscalar resonances $f_0(1370)$ and $f_0(1500)$ have been discovered [2, 3, 4, 5]; now these resonances are actively discussed in connection with the glueball problem. To establish the systematics of quark-antiquark states, the study of $p\bar{p}$ annihilation in flight carried out in 1999-2001 [6] was of a particular importance, for it allowed us to investigate the mass region 1900–2400 MeV: a large number of resonances discovered in this region made it possible to fix the $q\bar{q}$ trajectories on the (n, M^2) and (J, M^2) planes [1, 7]. We speak about the systematics of the $q\bar{q}$ states in Section 2 of this paper.

Scalar mesons play crucial role for understanding the strong QCD. Starting from 1995, the PNPI group worked upon the K-matrix fit to the wave ($IJ^{PC} = 00^{++}$) based on the simultaneous analysis of all data available by that time. The necessity of a combined analysis was dictated by the existence of large interference effects "resonance–background" as well as the effects associated with the resonance overlapping. In a situation of such a type, only a combined fitting to a large number of reactions allows one to hope for reliable results. In Section 3, a current understanding of scalar-meson sector is presented based on recent results of the K-matrix fit to meson spectra [8].

Previous analyses carried out in 1997–1998 [9, 10, 11] were based on the experimental data as follows:
(1) GAMS data on the S-wave two-meson production in the reactions $\pi p \to \pi^0\pi^0 n$, $\eta\eta n$ and $\eta\eta' n$ at small nucleon momenta transferred, $|t| < 0.2$ (GeV/c)^2 [12, 13];
(2) GAMS data on the $\pi\pi$ S-wave production in the reaction $\pi p \to \pi^0\pi^0 n$ at large momentum transfers squared, $0.30 < |t| < 1.0$ (GeV/c)^2 [12];
(3) BNL data on the reaction $\pi^- p \to K\bar{K} n$ [14];
(4) CERN-Münich data on $\pi^+\pi^- \to \pi^+\pi^-$ [15];
(5) Crystal Barrel data on $p\bar{p}$(at rest, from liquid hydrogen)$\to$ $\pi^0\pi^0\pi^0$, $\pi^0\pi^0\eta$, $\pi^0\eta\eta$ [3, 5, 16].

Now the experimental basis has much broadened, and additional samples of data are included into the analysis [8] of the 00^{++} wave as follows:
(6) Crystal Barrel data on proton-antiproton annihilation in gas: $p\bar{p}$(at rest, from gaseous hydrogen)$\to \pi^0\pi^0\pi^0$, $\pi^0\pi^0\eta$ [17],
(7) Crystal Barrel data on proton-antiproton annihilation in liquid: $p\bar{p}$(at rest, from liquid hydrogen)$\to \pi^+\pi^-\pi^0$, $K^+K^-\pi^0$, $K_SK_S\pi^0$, $K^+K_S\pi^-$ [17];
(8) Crystal Barrel data on neutron-antiproton annihilation in liquid deuterium: $n\bar{p}$(at rest, from liquid deuterium)$\to \pi^0\pi^0\pi^-$, $\pi^-\pi^-\pi^+$, $K_SK^-\pi^0$, $K_SK_S\pi^-$ [17];
(9) E852 Collaboration data on the $\pi\pi$ S-wave production in the reaction $\pi^-p \to \pi^0\pi^0n$ at the nucleon momentum transfers squared $0 < |t| < 1.5$ (GeV/c)^2 [18].

In addition to Ref. [9], the reactions of the $p\bar{p}$ annihilation in gas have been also included into the analysis [8]. One should keep in mind that in liquid hydrogen the $p\bar{p}$ annihilation is going dominantly from the S-wave state, while in gas there is a considerable admixture of the P-wave, thus giving an opportunity to analyse the three-meson Dalitz plots in more detail. New Crystal Barrel data allowed us to study the two-kaon channel with a more confidence as compared to what had been done before. This is undoubtedly important for the conclusion about the quark-gluon content of the scalar–isoscalar f_0-mesons under investigation.

Experimental data of the E852 Collaboration on the reaction $\pi^-p \to \pi^0\pi^0n$ at $p_{lab} = 18$ GeV/c [18] together with the GAMS data on the reaction $\pi^-p \to \pi^0\pi^0n$ at $p_{lab} = 38$ GeV/c [12] give us a solid ground for the study of the resonances $f_0(980)$ and $f_0(1300)$, for at large momenta transferred to the nucleon, $|t| \sim 0.5 \sim 1.5$ (GeV/c)^2, the production of resonances is accompanied by a small background, thus allowing us to fix reliably their masses and widths. This is especially important for $f_0(1300)$: in the compilation [19] this resonance is quoted as $f_0(1370)$, with the mass in the interval $1200 - 1500$ MeV, though experimental data favour rather definitely the mass near 1300 MeV.

The K-matrix amplitude determines both the amplitude poles (masses and widths of resonances) and K-matrix poles (masses of bare states). The K-matrix poles differ from the amplitude poles in two items:
(i) The states corresponding to the K-matrix poles do not contain any component associated with the decay processes, i.e. the transitions into real mesons. The absence of a cloud of real mesons allows us to refer conventionally to these states as bare ones [9, 11, 20].
(ii) Due to the transition *bare state(1)* $\to$ *real mesons* $\to$ *bare state(2)* the observed resonances are mixtures of bare states — in the first place this is related to the f_0-mesons. So, for quark systematics, the bare states are primary objects rather than the resonances.

This can be explained with the example of the behaviour of a level in the potential picture. Consider a potential well and the levels which correspond to stable states. Then gradually we switch the decay channels on, that is, replace impenetrable wall by potential barrier — at the beginning this leads to a broadening of levels, but masses

of states remain almost the same. But when the widths and resonance positions are such that resonances overlap, a cardinal reconstruction of the structure of levels occurs. Namely, one of resonances accumulates the widths of its resonance-neighbours thus making them comparatively narrow. In this way an intensive mixing of resonance states takes place, while the positions of masses are shifted in a value of the order of the resonance width, in 100–200 MeV. The K-matrix amplitude allows us to trace the transformation of stable levels (bare states) into resonances. The K-matrix amplitude works with parameters related to stable levels. Multichannel unitarization of the amplitude, which is inherent in the K-matrix representation, with the account for analyticity, allows one to trace the transformation of stable levels into real resonances. A characteristic feature of the K-matrix fit is its ability to reconstruct the picture of stable levels as well as re-create a real picture of complex masses and partial widths.

The latest K-matrix fit [8] gave us rather definite information on the resonances $f_0(980)$, $f_0(1300)$, $f_0(1500)$, $f_0(1750)$ and broad state $f_0(1200-1600)$. Relying on the extracted partial widths for transitions to the channels $\pi\pi, K\bar{K}, \eta\eta, \eta\eta'$, one can analyse the quark-gluonium content of these states. In this way the following properties of resonances are to be formulated:

1. $f_0(980)$: This resonance is dominantly the $q\bar{q}$ state, $q\bar{q} = n\bar{n}\sin\varphi + s\bar{s}\cos\varphi$, with a large $s\bar{s}$ component. Assuming the glueball admixture to be not greater than 20%, $W_{gluonium} \lesssim 20\%$, the hadronic decays give us the following constraints for mixing angle: $-95^\circ \leq \varphi \lesssim -40^\circ$. Rather large uncertainties in the determination of mixing angle are due to a high sensitivity of coupling constants to a plausible small admixture of the gluonium. At $W_{gluonium} = 0$, hadronic decays provide us with $\varphi = -67^\circ \pm 10^\circ$.

2. $f_0(1300)$ (in the compilation [19] this resonance is denoted as $f_0(1370)$): This resonance is the descendant of the bare $q\bar{q}$ state which is close to the flavour singlet. The resonance $f_0(1300)$ is formed due to a strong mixing with the primary gluonium and neighbouring $q\bar{q}$ states. The quark-antiquark content of $f_0(1300)$, $q\bar{q} = n\bar{n}\cos\varphi + s\bar{s}\sin\varphi$ determined from the transitions $f_0(1300) \to \pi\pi, K\bar{K}, \eta\eta$ strongly depends on the admixture of the gluonium component. At $W_{gluonium} \lesssim 30\%$ the mixing angle changes, depending on $W_{gluonium}$ and interference sign, in the interval $-45^\circ \lesssim \varphi[f_0(1300)] \lesssim 25^\circ$; at $W_{gluonium} = 0$ the hadronic decays provide us $\varphi[f_0(1300)] = -6^\circ \pm 10^\circ$.

3. $f_0(1500)$: This resonance is the descendant of a bare state with large $n\bar{n}$ component. Like $f_0(1300)$, the resonance $f_0(1500)$ is formed by mixing with the gluonium and neighbouring $q\bar{q}$ states. The quark-antiquark content, $q\bar{q} = n\bar{n}\cos\varphi + s\bar{s}\sin\varphi$, depends on the admixture of the gluonium: at $W_{gluonium} \lesssim 30\%$ the mixing angle changes, depending on $W_{gluonium}$, in the interval $-20^\circ \lesssim \varphi[f_0(1300)] \lesssim 25^\circ$; at $W_{gluonium} = 0$ one has $\varphi[f_0(1500)] = 11^\circ \pm 8^\circ$.

4. $f_0(1750)$: This resonance is the descendant of the bare state belonging to the radial-excitation nonet $2^3P_1 q\bar{q}$, the wave function of which has large $s\bar{s}$ component. The K-matrix analysis permits the two solutions, with different values of the $s\bar{s}$ component. In the first solution, the $s\bar{s}$ component dominates; in the absence of gluonium

component, $\varphi[f_0(1750)] = -72^\circ \pm 5^\circ$, and if the gluonium admixture does not exceed 30%, then $-110^\circ \lesssim \varphi[f_0(1750)] \lesssim -35^\circ$. In the second solution, in the absence of gluonium component, $\varphi[f_0(1750)] = -18^\circ \pm 5^\circ$, and with the gluonium admixture $W_{gluonium} \lesssim 30\%$, $-50^\circ \lesssim \varphi[f_0(1750)] \lesssim 10^\circ$.

5. $f_0(1200-1600)$: The broad state is the descendant of the primary glueball. The analysis of hadronic decays of this resonance confirmed its glueball nature: the glueball descendant has the quark-antiquark component $(q\bar{q})_{glueball} = (u\bar{u}+d\bar{d}+\sqrt{\lambda}s\bar{s})/\sqrt{2+\lambda}$ [21], which is defined by the probability to create new $q\bar{q}$-pairs by the gluon field $u\bar{u} : d\bar{d} : s\bar{s} = 1 : 1 : \lambda$, the suppression parameter for the production of strange quarks being in the interval $\lambda \simeq 0.5 - 0.8$ [22, 23]. In terms of mixing angle for the $n\bar{n}$ and $s\bar{s}$ components, this means that the glueball descendant must have $\varphi_{glueball} \simeq 27^\circ - 33^\circ$, and just these values for $\varphi[f_0(1200-1600)]$ have been obtained in all variants of the K-matrix fit [8]. Such a value of mixing angle, $\varphi[f_0(1200-1600)] = 30^\circ \pm 3^\circ$, does not allow one to determine the admixture of the $q\bar{q}$ component in the broad state. This is due to the fact that the $(q\bar{q})_{glueball}$ and gluonium components are coupled to the channels $\pi\pi, K\bar{K}, \eta\eta$ and $\eta\eta'$ in equal proportions.

Referring to the broad state $f_0(1200-1600)$ as a resonance needs some comments. The observed spectra in the channels $\pi\pi, K\bar{K}, \eta\eta, \eta\eta'$ demand to introduce a broad bump, and it occurred that this bump behaves in a universal way, thus enabling us to describe it as a resonance state. Indeed, a characteristic feature of the resonance is the factorization property: the resonance amplitude may be represented in the form $g_{in}(s-M^2)^{-1}g_{out}$, and universal constants g_{in} and g_{out} depend on the sort of initial and final states only. The description of a large number of reactions in [8] agrees well with the factorization property of the broad-state amplitude. A large width of the $f_0(1200-1600)$ does not allow us to determine reliably its mass, but due to a strong production of the $f_0(1200-1600)$ in a large number of reactions we can, with a confidence, to find out the ratio of couplings to the channels $\pi\pi, K\bar{K}, \eta\eta, \eta\eta'$, that is, to define its content in terms of the $q\bar{q}$ and gluonium states.

The K-matrix [8] analysis does not point determinedly to the existence of the light σ-meson which is actively discussed at present (e.g. see [24] and references therein), in particular in connection with the recently reported signals in the $\pi\pi$ spectra of the decays $D^+ \to \pi^+\pi^+\pi^-$ (pole in the amplitude at $M = (480 \pm 40) - i(160 \pm 30)$ MeV [25]), $J/\Psi \to \pi\pi\omega$ (pole at $M = (390\,^{+60}_{-36}) - i(141\,^{+38}_{-25})$ MeV [26]), $\tau \to \pi\pi\pi\nu$ (pole at $M \simeq 555 - i270$ MeV [27]). Possible explanation of this discrepancy may consist in a strong suppression of the light σ-meson production in the $p\bar{p}$ annihilation processes, like $p\bar{p} \to \pi\pi\pi$, though, as one may think, there is no visible reason for such a suppression. Recall that the statistics in the Crystal Barrel reactions is by two orders of magnitude larger than in [25, 26, 27]. Alternative explanation can be associated with a restricted applicability of the K-matrix approach at small invariant energy squared s: the K-matrix amplitude does not describe properly the left-hand singularities associated with meson exchanges in the crossing channels. So one may suppose that the K-matrix analysis does not reconstruct analytical amplitude correctly at $\mathrm{Re}\, s \lesssim 4m_\pi^2$, i.e. at $(\mathrm{Re}\, M)^2 - (\mathrm{Im}\, M)^2 \lesssim 4m_\pi^2$, $(\mathrm{Re}\, M)^2 - (\mathrm{Im}\, M)^2 \lesssim 4m_\pi^2$. In

numerous analyses, including those carried out in the dispersion relation technique where left-hand cuts can be accounted for in one way or another, the pole ascribed to the light σ-meson occurred just at $\mathrm{Re}\, s \lesssim 4m_\pi^2$, e.g. see [28, 29, 30, 31]. In this connection let us emphasize that the dispersion-relation N/D analysis [31], where the low-energy 00^{++} amplitude was sewed with the K-matrix amplitude [9], leads to the pole at $M \simeq 430 - i325$ MeV.

Therefore, the K-matrix amplitude analysis tells us that in the scalar–isoscalar sector there are two states, the broad resonance $f_0(1200-1600)$ and the light sigma-meson $f_0(300-500)$, which are extra ones for the $q\bar{q}$-systematics of mesons. In the final Section 4, the status of these possible exotic states is discussed as well as two more candidates for exotics — $\pi_2(1880)$ and the $(J^{PC} = 1^{-+})$ state (recall that $q\bar{q}$-system cannot have such quantum numbers).

2 Experimental data of the Crystal Barrel Collaboration and systematics of mesons states

In 1989-1997, the Crystal Barrel Collaboration studied the reactions of the $p\bar{p}$-annihilation at rest and in flight at LEAR (CERN), that resulted in the accumulation of a huge statistics on multi-meson states. However, initially the analysis of experimental data had not been carried out in due course. The first attempt to analyse pion spectra in the reaction $p\bar{p}$ (at rest) $\to \pi^0\pi^0\pi^0$ based on a simplified isobar model led to a wrong identification of the peak near 1500 MeV; the peak had been identified as the tensor meson AX(1515) [32], and at the same time no scalar states were seen in the $\pi\pi$ spectra over the range 1200–1700 MeV.

In reactions such as $p\bar{p}$ (at rest) $\to \pi^0\pi^0\pi^0$ the three-particle interaction characteristics reveal themselves in full scale, that should be accounted for in the analysis of meson spectra. The method based on the extraction of leading singularities (pole, square root, logarithmic ones, and so on) in the production amplitude of a few particles was developed in the papers [33, 34, 35]. This method had been applied with the purpose to re-analyse the Crystal Barrel data for the reaction $p\bar{p}$ (at rest) $\to \pi^0\pi^0\pi^0$, and in the work performed together with the Collaboration members, the resonances $f_0(1370)$ and $f_0(1500)$ had been discovered in the region 1300–1500 MeV [2, 3, 4]. The data on the reactions $p\bar{p} \to \pi^0\pi^0\eta$ and $p\bar{p} \to \pi^0\eta\eta$ involved into combined analysis enabled us to discover a group of tensor and scalar-isovector resonances [5]. The masses and widths of these resonances obtained in the latest analysis are shown in Table 1, and the analysed reactions are quoted in Table 2.

A combined fit to data collected in various reactions and experiments is a specific feature of the method used in the papers [8, 9, 10]. The matter is that, because of the presence of a considerable reaction background, the resonance does not always reveal itself as a peak in meson spectrum: due to interference effects the resonance may appear as a dip in the spectrum, or it may be seen as a "shoulder". Including into analysis

the GAMS data on the two-meson spectra in the reactions $\pi^- p \to \pi^0\pi^0 n$, $\pi^- p \to \eta\eta n$, $\pi^- p \to \eta\eta' n$ [12, 13], BNL data on $\pi^- p \to K^+K^- n$ [14] and CERN–Münich data on $\pi^- p \to \pi^+\pi^- n$ [15] allowed us not only to determine reliably the ratios of different two-meson yields (that is rather important for the resonance classification), but also to conclude that the peak in the $\eta\eta$-spectrum in the reaction $\pi^- p \to \eta\eta n$, which was previously claimed to be the resonance $G(1590)$ [13], appeared in fact as a result of the interference of the broad state $f_0(1200-1600)$ and $f_0(1500)$ resonance [36].

Table 1: Resonances discovered in the analysis of Crystal Barrel data. Masses and widths are presented in accordance with the latest combined analysis [1,8]

Resonance	$I^G J^{PC}$	Mass, MeV	Width, MeV
$f_0(1300)$ (or $f_0(1370)$ [21])	0^+0^{++}	1310 ± 20	280 ± 30
$f_0(1500)$	0^+0^{++}	1495 ± 6	126 ± 5
$f_0(1200-1600)$	0^+0^{++}	1400 ± 200	1200 ± 400
$a_0(1450)$	1^-0^{++}	1520 ± 25	240 ± 20
$a_2(1660)$	1^-2^{++}	1670^{+40}_{-20}	310 ± 40
$f_2(1565)$	0^+2^{++}	1580 ± 6	160 ± 20

Table 2: The list of reactions used in the combined analysis [1,8]

Crystal Barrel reactions	Two-particle data	
	Reaction	Collaboration
$\bar{p}p \to \pi^0\pi^0\pi^0$	$\pi^- p \to \pi^-\pi^+ n$	CERN- Münich
$\bar{p}p \to \eta\pi^0\pi^0$	$\pi^- p \to \pi^0\pi^0 n$	GAMS
$\bar{p}p \to \eta\eta\pi^0$	$\pi^- p \to \eta\eta n$	GAMS
$\bar{p}p \to \pi^+\pi^-\pi^0$	$\pi^- p \to \eta\eta' n$	GAMS
$\bar{p}n \to \pi^+\pi^-\pi^-$	$\pi^- p \to K\bar{K}n$	BNL
$\bar{p}n \to \pi^-\pi^0\pi^0$	$\pi^- p \to \pi^0\pi^0 n$	E852
$\bar{p}p \to \pi^0 K_S K_S$		
$\bar{p}p \to \pi^0 K^+ K^-$		
$\bar{p}p \to \pi^+ K^- K_S$		
$\bar{p}n \to \pi^- K_S K_S$		
$\bar{p}n \to \pi^0 K^- K_S$		

Table 3: Resonances discovered in the analysis of the $p\bar{p}$-annihilation reactions in flight [6]. One star means that the resonance had been observed in one reaction only or it reveals itself poorly. Two stars mean that the resonance was seen in two reactions or in one where its contribution dominates. Three stars mark well-established resonances by using several reactions.

Resonance	I^GJ^{PC}	Mass, MeV	Width, MeV	Status of the state
π	1^-0^{-+}	2070 ± 35	310 ± 80	*
π	1^-0^{-+}	2360 ± 30	300 ± 80	*
a_1	1^-1^{++}	2270 ± 50	300 ± 70	*
π_2	1^-2^{-+}	2005 ± 20	210 ± 40	*
π_2	1^-2^{-+}	2245 ± 60	320 ± 60	*
a_2	1^-2^{++}	1950 ± 40	180 ± 40	**
a_2	1^-2^{++}	2030 ± 20	205 ± 30	***
a_2	1^-2^{++}	2175^{+80}_{-30}	310 ± 60	*
a_2	1^-2^{++}	2255 ± 20	230 ± 15	***
a_3	1^-3^{++}	2030 ± 20	150 ± 20	**
a_3	1^-3^{++}	2275 ± 40	150 ± 20	*
a_4	1^-4^{++}	2005 ± 30	180 ± 30	***
a_4	1^-4^{++}	2255 ± 40	330 ± 70	**
π_4	1^-4^{-+}	2250 ± 15	215 ± 25	**
f_0	0^+0^{++}	2105 ± 15	200 ± 25	**
f_0	0^+0^{++}	2320 ± 30	175 ± 45	*
f_2	0^+2^{++}	1920 ± 40	260 ± 40	**
f_2	0^+2^{++}	2020 ± 30	275 ± 35	***
f_2	0^+2^{++}	2240 ± 30	245 ± 45	***
f_2	0^+2^{++}	2300 ± 35	290 ± 50	**
f_4	0^+4^{++}	2020 ± 25	170 ± 20	***
f_4	0^+4^{++}	2300 ± 25	280 ± 50	**
η_2	0^+2^{-+}	2030 ± 40	190 ± 40	**
η_2	0^+2^{-+}	2250 ± 40	270 ± 40	***
ω	0^-1^{--}	2150 ± 20	235 ± 30	**
ω	0^-1^{--}	2295 ± 50	380 ± 60	*
ω_2	0^-2^{--}	1975 ± 20	175 ± 25	*
ω_2	0^-2^{--}	2195 ± 30	225 ± 40	*
ω_3	0^-3^{--}	1960 ± 30	165 ± 30	**
h_1	0^-1^{+-}	2000 ± 20	205 ± 20	**
h_1	0^-1^{+-}	2270 ± 15	175 ± 30	**
ρ_1	1^+1^{--}	1980 ± 30	165 ± 30	**
ρ_2	1^+2^{--}	1940 ± 40	155 ± 40	*
ρ_2	1^+2^{--}	2225 ± 35	335 ± 75	*
ρ_3	1^+3^{--}	1980 ± 15	175 ± 20	**
ρ_3	1^+3^{--}	2260 ± 20	200 ± 30	*
ρ_4	1^+4^{--}	2240 ± 25	210 ± 40	**
b_1	1^+1^{+-}	1970 ± 40	215 ± 60	**
b_1	1^+1^{+-}	2210 ± 50	275 ± 45	*
b_3	1^+3^{+-}	2020 ± 15	110 ± 20	**
b_3	1^+3^{+-}	2245 ± 50	350 ± 80	*

The data by the Crystal Barrel Collaboration discussed above were obtained from the $p\bar{p}$-annihilation at rest. In addition, the Crystal Barrel Collaboration has a huge statistics for the events of the $p\bar{p}$-annihilation in flight, the antiproton momentum covering the range 600–1900 MeV. After the Crystal Barrel Collaboration stopped its activity in 1999, these data were provided to the PNPI group for further processing and analysis of spectra. In 1999–2001, together with the colleagues from Queen Mary and Westfield College (London) and Rutherford–Appleton Laboratory, the PNPI group analysed these data. More than thirty resonances have been discovered in the mass range 1900–2400 MeV [6]; they are shown in Table 3. The discovery of these resonances allowed us to establish systematics of meson $q\bar{q}$-states on the (n, M^2)- and (J, M^2)-planes [1, 7] (n is radial quantum number of the $q\bar{q}$-state with mass M and J is its spin).

2.1 Systematics of meson states

In Figs. 1 and 2, the trajectories on the (n, M^2)- and (I, J^{PC})-planes are shown for the states with negative and positive charge parities:

$$\begin{aligned} C\ =\ -: &\quad b_1(11^{+-}),\ b_3(13^{+-}),\ h_1(01^{+-}),\ \rho(11^{--}),\ \rho_3(13^{--}),\\ &\quad \omega/\phi(01^{--}),\quad \omega_3(03^{--})\ ; \qquad (1)\\ C\ =\ +: &\quad \pi(10^{-+}),\ \pi_2(12^{-+}),\ \pi_4(14^{-+}),\ \eta(00^{-+}),\ \eta_2(02^{-+}),\\ &\quad a_0(10^{++}),\ a_1(11^{++}),\ a_2(12^{++}),\ a_3(13^{++}),\ a_4(14^{++}),\\ &\quad f_0(00^{++}),\quad f_2(02^{++})\ . \qquad (2) \end{aligned}$$

In terms of $q\bar{q}$-states, the mesons of the nonets $n^{2S+1}L_J$ fill in the following (n, M^2)-trajectories for $M \lesssim 2400\,\mathrm{MeV}$:

$$\begin{aligned} &{}^1S_0\ \to\ \pi(10^{-+}),\ \eta(00^{-+})\ ; \qquad (3)\\ &{}^3S_1\ \to\ \rho(11^{--}),\ \omega(01^{--})/\phi(01^{--})\ ;\\ &{}^1P_1\ \to\ b_1(11^{+-}),\ h_1(01^{+-})\ ;\\ &{}^3P_J\ \to\ a_J(1J^{++}),\ f_J(0J^{++}),\ J=0,1,2\ ;\\ &{}^1D_2\ \to\ \pi_2(12^{-+}),\ \eta_2(02^{-+})\ ;\\ &{}^3D_J\ \to\ \rho_J(1J^{--}),\ \omega_J(0J^{--})/\phi_J(0J^{--}),\ J=1,2,3\ ;\\ &{}^1F_3\ \to\ b_3(13^{+-}),\ h_3(03^{+-})\ ;\\ &{}^3F_J\ \to\ a_J(1J^{++}),\ f_J(0J^{++}),\ J=2,3,4\ . \end{aligned}$$

Different orbital momenta can form the trajectories with the same J, namely, $J = L \pm 1$. Therefore, the number of such trajectories doubles; these states are $(I, 1^{--})$, $(I, 2^{++})$, and so on. Isoscalar states have two flavour components $n\bar{n} = (u\bar{u} + d\bar{d})/\sqrt{2}$ and $s\bar{s}$, that also results in a doubling of trajectories such as $\eta(00^{-+})$, $f_0(00^{++})$, and so on.

The trajectories with negative charge parity, $C = -$, can be defined practically unambigously (in Figs. 1 and 2, black circles stand for the observed states [6, 8, 19], while open circles mark the states predicted by trajectories). The trajectories are linear with a good accuracy:

$$M^2 \ \simeq \ M_0^2 + (n-1)\mu^2 \ , \tag{4}$$

where M_0 is the mass of the basic meson with $n = 1$, and the slope parameter is about $\mu^2 \simeq 1.3\,\mathrm{GeV}^2$. The trajectory slopes for $b_1(11^{+-})$ and $b_3(13^{+-})$ are slightly lower: for them $\mu^2 \simeq 1.2\,\mathrm{GeV}^2$.

In the sector with $C = +$, the states π_J belong definitely to linear trajectories with $\mu^2 \simeq 1.2\,\mathrm{GeV}^2$, with an exception for $\pi(140)$ that is not a surprise, for the pion is rather specific state. The sector of the a_J-states with $J = 0, 1, 2, 3, 4$ demonstrates a neat set of linear trajectories, with the slopes $\mu^2 \simeq 1.15 - 1.20\,\mathrm{GeV}^2$; the same slope is seen for the f_2- and f_4-trajectories.

For the f_0-mesons the trajectory slope is $\mu^2 \simeq 1.3\,\mathrm{GeV}^2$. Let us emphasize that two states do not lay on linear $q\bar{q}$-trajectories, namely, the light σ-meson $f_0(300-500)$ [19] and the broad state $f_0(1200-1600)$, this latter has been fixed by the K-matrix analysis [8, 9, 10].

The picture of the state location on the (n, M^2)-plot is complemented by trajectories on the (J, M^2)-plots: they are shown in Fig. 3. To draw the daughter (J, M^2) trajectories, it was important that leading meson trajectories ($\pi, \rho, , a_1, a_2$ and P') were well-known from the analysis of hadronic diffractive scatterings at $p_{lab} \sim 5-50$ GeV/c.

Pion trajectories, leading and daughter ones, are linear with a good accuracy, see Fig. 3. The other leading trajectories, $\rho, \eta, a_1, a_2, f_2$ or P', can be also considered as linear, with a good accuracy:

$$\alpha_X(M^2) \ \simeq \ \alpha_X(0) + \alpha'_X(0) M^2 \ . \tag{5}$$

The parameters of linear trajectories determined by masses of the $q\bar{q}$-states are as follows:

$$\begin{array}{ll}
\alpha_\pi(0) \simeq -0.015 \ , & \alpha'_\pi(0) \simeq 0.72 \ \mathrm{GeV}^{-2}; \\
\alpha_\rho(0) \simeq 0.50 \ , & \alpha'_\rho(0) \simeq 0.83 \ \mathrm{GeV}^{-2}; \\
\alpha_\eta(0) \simeq -0.24 \ , & \alpha'_\eta(0) \simeq 0.80 \ \mathrm{GeV}^{-2}; \\
\alpha_{a_1}(0) \simeq -0.10 \ , & \alpha'_{a_1}(0) \simeq 0.72 \ \mathrm{GeV}^{-2}; \\
\alpha_{a_2}(0) \simeq 0.45 \ , & \alpha'_{a_2}(0) \simeq 0.91 \ \mathrm{GeV}^{-2}; \\
\alpha_{P'}(0) \simeq 0.71 \ , & \alpha'_{P'}(0) \simeq 0.83 \ \mathrm{GeV}^{-2}.
\end{array} \tag{6}$$

The slopes of the $\alpha'_X(0)$ trajectories are approximately the same. The inverse slope value, $1/\alpha'_X(0) \simeq 1.25 \pm 0.15\,\mathrm{GeV}^2$, is of the order of the slope μ^2 for the trajectories on the (n, M^2)-plane:

$$\frac{1}{\alpha'_X(0)} \ \simeq \ \mu^2 \ . \tag{7}$$

The daughter trajectories for π (Fig. 3a), a_1 (Fig. 3b), ρ (Fig. 3c), a_2 (Fig. 3d) and η (Fig. 3e) are determined unambigously. On the P'-trajectories, leading and daughter ones (Fig. 3f), there is no room for the states $f_0(300-500)$ and $f_0(1200-1600)$: this fact stresses once again that these states are superfluous for the $q\bar{q}$-systematics, i.e. they are exotic states.

2.2 Exotics — the states which do not belong to the quark-antiquark trajectories

As is seen, there are two states in the scalar-isoscalar sector which do not belong either to the (n, M^2) or (J, M^2) trajectories; these are the broad state $f_0(1200-1600)$, which was found in the K-matrix analysis of the 00^{++}-wave [8, 9, 10], and the light σ-meson.

The problem of the light σ-meson is discussed rather long ago [19, 28, 29, 30, 31], yet, until now, there is no common opinion about the existence of this state.

Recently there appeared indications that a signal from σ-meson has been seen in the reactions $D^+ \to \pi^+\pi^+\pi^-$ [25], $J/\psi \to \pi\pi\omega$ [26] and $\tau \to \pi\pi\pi\nu$ [27]. Nevertheless, one cannot state that it was a reliable experimental identification of this state, because in the three-particle spectra, in the region of small $\pi\pi$-masses, an enhancement of the spectra can occur, due to both reflected signals from other channels and the rescattering effects associated with the resonance production in other channels (triangle singularity effect [34, 35]). To single out these effects rather large statistics is necessary, comparable with that for the reactions investigated by Crystal Barrel; however, in the works [25, 26, 27] such a level of statistics had not been reached. Let us stress that the effects of reflected signals and those of triangle singularities were seen, when the Crysrtal Barrel reactions have been analysed, and for certain reactions they occurred to be rather important. Indeed, a correct identification of $f_0(1500)$ in the reactions $p\bar{p} \to \pi^0\pi^0\pi^0$, $\pi^0\eta\eta$ [2, 3, 4] became plausible after accounting for the interference of the decay $f_0(1500) \to \pi\pi, \eta\eta$ and reflected resonance signals from other channels; the triangle-diagram effects were also studied by analysing the reactions $p\bar{p} \to \pi^0\pi^0\pi^0, \pi^0\eta\eta$, see [2, 4], but it occurred that they do not affect the spectra directly, and they may be effectively described by introducing complex-valued parameters for resonance production. Still, in certain cases the triangle diagrams cannot be taken into account in such a simple way: another reaction investigated by Crystal Barrel, that is, $p\bar{p} \to \eta\pi^+\pi^-\pi^+\pi^-$ [37], where singular terms are located near the physical region, provided us with an example of strongly affected spectra. One can expect noticeable corrections coming from triangle diagramms also in the reactions $D^+ \to \pi^+\pi^+\pi^-$, $J/\psi \to \pi\pi\omega$ and $\tau \to \pi\pi\pi\nu$, for the effect of triangle diagrams is enhanced just near the small $\pi\pi$-masses, for more detail see [34, 35].

It is necessary to underline that in the reactions measured by Crystal Barrel the bumps in the $\pi\pi$-spectra are observed, which may be considered, owing to incorrect treatment, as an indication to the light σ-meson. The reaction $d\bar{p}$(at rest) $\to \pi^0\pi^0\pi^-$ can serve us as an example (see [8], Fig. 5): in the $\pi^0\pi^0$-spectrum, there is an obvious

enhancement over the phase space in the region $M_{\pi^0\pi^0} \sim 400 - 500\,\mathrm{MeV}$. However, the Dalitz-plot analysis proved that this enhancement is due to the reflected signal from $\rho(1450) \to \pi^-\pi^0$. The existence of a reflected signal in the $D^+ \to \pi^+\pi^+\pi^-$ is also possible [38].

To summarize, for the experimental discovery of the light σ-meson the data are needed, which would exceed the present statistics by one–two orders of value, i.e. it must be the statistics comparable with that of the Crystal Barrel reactions.

In the paper [39], the observation of the resonance $\pi_2(1880)$ was reported; this state does not belong to (n, M^2)- and (J, M^2)-trajectories. Being an extra state for the $q\bar{q}$-systematics, the $\pi_2(1880)$ can be the hybrid: the $q\bar{q}g$-system.

3 Scalar-meson sector

In this Section, the results of the K-matrix analyses performed in [8, 9] for the scalar sector are subsequently presented. The sector of scalar mesons is of a particular interest; a variety of opinions exist concerning the properties of states which belong to this sector, e.g., see [11, 40, 41, 42, 43, 44, 45]. The latest analysis [8] is the most detailed investigation of the 00^{++} wave, where the available data have been used in a full scale.

3.1 The K-matrix analysis of the $(IJ^{PC} = 00^{++})$-wave

In a set of papers [8, 9, 10, 20], the K-matrix analysis of the waves $IJ^{PC} = 00^{++}$, 10^{++}, 02^{++}, 12^{++} had been carried out in the mass range 280–1900 MeV. For these states, the masses and widths of resonances had been found. In the scalar–isoscalar sector the following states are seen (see Fig. 4):

$$\begin{aligned} 00^{++}: \qquad & f_0(980),\ f_0(1300),\ f_0(1500)\ , \\ & f_0(1200-1600),\ f_0(1750)\ . \end{aligned} \tag{8}$$

The $f_0(980)$ is a well-known resonance, its properties and its nature are intensively discussed during several decades. The $f_0(1300)$ resonance is denoted in the compilation [19] as $f_0(1370)$, however its mass following the most accurate determination, as is stressed above, is near 1300 MeV — so the notation $f_0(1300)$ is used here. The $f_0(1500)$ resonance had been discovered in [2, 3, 4], now it is a well-established state. A few years ago, there existed a strong belief that in the region around 1700 MeV a comparatively narrow state, $f_J(1710)$, was present, with $J = 0$ or 2. The K-matrix analysis [8, 9, 10, 20] points to the existence of $f_0(1750)$, with the width $\Gamma \sim 140 - 300$ MeV: the uncertainty in the definition of the width of $f_0(1750)$ is due to a bad knowledge of the $\pi\pi\pi\pi$ channel in this mass range and, correspondingly, with two available solutions, with $\Gamma \sim 140\,\mathrm{MeV}$ and $\Gamma \sim 300\,\mathrm{MeV}$.

The broad state $f_0(1200 - 1600)$, with a half-width $500 - 900$ MeV, is definitely needed for the K-matrix analysis. In the paper [9] this state had been denoted as

$f_0(1530^{+90}_{-250})$: a large error in the definition of the mass is due to the remoteness of the pole from the real axis (physical region) as well as to the existence of several solutions given by the K-matrix analysis.

A large number of reactions, which were succefully described with the $f_0(1200-1600)$, proved the valididty of a factorization inherent in the resonance amplitude: near the pole the amplitude is $g_{in}(s-M^2)^{-1}g_{out}$, where the universal coupling constants, g_{in} and g_{out}, depend on the type of the intial and final states only. A strong production of the $f_0(1200-1600)$ in various processes allows one to fix reliably these coupling constants.

In the scalar–isovector sector, the K-matrix analysis points to the presence of two resonances:

$$10^{++}: \quad a_0(980),\ a_0(1520)\ , \tag{9}$$

while in the tensor-meson sector the following states are seen:

$$\begin{aligned} 12^{++} &: \qquad a_2(1320),\ a_2(1660)\ ; \\ 02^{++} &: \qquad f_2(1270),\ f_2(1525),\ f_2(1580)\ . \end{aligned} \tag{10}$$

3.1.1 K-matrix amplitude

In the K-matrix analysis, the fitting parameters are the K-matrix elements which are represented as the sums of pole terms $g_a^{(n)}g_b^{(n)}/(\mu_n^2-s)$ ($s\equiv M^2$ is the invariant energy squared of mesons, $s\equiv M^2$) and a smooth s-dependent term $f_{ab}(s)$. Namely,

$$K_{ab} \ = \ \sum_n \frac{g_a^{(n)}g_b^{(n)}}{\mu_n^2-s} + f_{ab}(s)\ , \tag{11}$$

where fitting parameters are $g_a^{(n)}$, μ_n and f_{ab}, and the indices a,b refer to the reaction channels: $f_0\to\pi\pi, K\bar{K}, \eta\eta, \eta\eta'$ and $\pi\pi\pi\pi$. The K-matrix poles are not the amplitude poles, i.e. they do not correspond to real states. The amplitude in the K-matrix approach is written as follows:

$$\widehat{A} \ = \ \frac{\widehat{K}}{1-i\hat{\rho}\widehat{K}}\ , \tag{12}$$

where $\hat{\rho}$ is the diagonal matrix of phase spaces for the processes under consideration, $\hat{\rho}=\mathrm{diag}\,(\rho_1(s),\rho_2(s),...)$. Because of that, the amplitude poles correspond to the zeros of the determinant:

$$\det\left|1-i\hat{\rho}\widehat{K}\right| \ = \ 0\ , \tag{13}$$

while the K-matrix poles respond to the states with switched-off decay channels. The states associated with the K-matrix poles do not contain a cloud of real mesons which appear during resonance decay: this circumastance allows one to call the K-matrix poles the "bare states" [9, 11, 20, 36].

3.1.2 Partial amplitude for the 00^{++} wave: unitarity, analyticity and the problem of the left-hand cut

The K-matrix representation of partial amplitude takes account of the well-known fact that at low and moderate energies the inelastic processes are dominantly two-particle ones. Being applied to the 00^{++} wave this means that, along with the elastic scattering $\pi\pi \to \pi\pi$ (threshold at $\sqrt{s} = 280\,\mathrm{MeV}$), we have the transitions $\pi\pi \to K\bar{K}$ (threshold at $\sqrt{s} = 2m_K$), $\pi\pi \to \eta\eta$ and $\pi\pi \to \eta\eta'$ (thresholds at $\sqrt{s} = 2m_\eta$ and $\sqrt{s} = m_\eta + m_{\eta'}$). Besides, in the 00^{++}-wave at $\sqrt{s} \gtrsim 1300 - 1400\,\mathrm{MeV}$, a considerable four-pion production is observed, but this process can be also treated, with a good accuracy, as a formation of two ρ's or two effective σ-mesons: $\pi\pi \to \rho\rho \to \pi\pi\pi\pi$ and $\pi\pi \to \sigma\sigma \to \pi\pi\pi\pi$. The amplitude in the K-matrix representation takes into account correctly both unitarity and threshold singularities for the two-meson processes. In this way, the K-matrix representation of the amplitude serves us as a right frame for the correct reconstruction of the amplitude above the $\pi\pi$ threshold (in our case, over the range 280–1900 MeV).

In the K-matrix amplitude, the threshold singularities are taken into account by treating the phase spaces as analytical functions of the total energy squared s: above the threshold, the two-particle phase space can be represented in a standard form $\rho_a(s) = \sqrt{1 - (m_{1a} + m_{2a})^2/s}$, and below threshold it should be expressed through analytical continuation: $\rho_a(s) = i\sqrt{(m_{1a} + m_{2a})^2/s - 1}$. The phase space of the two-resonance state, of the type of $\rho\rho$ or $\sigma\sigma$, may be expressed in the form which reproduces correctly the threshold singularities, namely, threshold singularity at $\sqrt{s} = 4m_\pi$ and the singularity in the lower complex half-plane s (on the third sheet) at $\sqrt{s} = 2(m_\rho - i\Gamma_\rho/2)$, that is related to the production of $\rho\rho$, see [8, 9, 11] for more detail.

The singularities, which are not explicitly taken into account within the K-matrix approach, are the so-called left-hand side singularities of the partial amplitude. These singularities are due to the exchange of particles in the crossing channels (i.e. in the t- and u-channels), they determine the interaction forces. In the $\pi\pi$-scattering amplitude, the nearest left singularity is located at $s = 0$; this singularity is associated with the two-pion exchanges in the t- and u-channels. A large contribution is provided by the ρ-meson exchange, that leads to the logarithmic singularity of the partial amplitude at $s = 4m_\pi^2 - m_\rho^2 \simeq -0.5\,\mathrm{GeV}^2$. In this very region, the two-pion exchange in the 00^{++} wave, that corresponds to the effective σ-meson, contributes significantly too. The contribution of tensor-meson exchanges is important in the region $s \simeq -1.5\,\mathrm{GeV}^2$.

The problem of a correct account for left-hand singularities becomes even more complicated, for the contributions from various exchanges cancel each other at small s to a great extent [46], so the contribution from the left-hand cut depends strongly on the details of the t- and u-channel exchange mechanism, in particular on the structure of the $\rho, \sigma, f_2 \to \pi\pi$ form factors.

Because of uncertainties in choosing the interaction forces, it would be reasonable not to inflict any hypothesis about the left-hand cut for the $\pi\pi$-scattering amplitude,

but to allow a freedom for the fitting procedure. The K-matrix technique, which was used in [8, 9], allows one to do that: this technique may be easily generalized in a way that enables to take account of the left-hand amplitude singularities. This opportunity was used in [8, 9], according to what the data require; this is an important item, let us discuss it in more detail.

By discussing the left-hand cut of the 00^{++}-amplitude, it is sufficient to restrain our consideration by one, the nearest, $\pi\pi$ channel only. In this case, partial amplitude can be written as follows:

$$A(s) \;=\; \frac{N(s)}{1-B(s)}\;, \tag{14}$$

where the pion loop diagram, which ensures the unitarity of the partial amplitude, is

$$B(s) \;=\; \int\limits_{4m_\pi^2}^{\infty} \frac{ds'}{\pi}\;\frac{N(s')\rho_{\pi\pi}(s')}{s'-s-i0}\;. \tag{15}$$

At $s > 4m_\pi^2$, the imaginary part of the loop diagram is $\mathrm{Im}\, B(s) = \rho_{\pi\pi}(s)N(s)$ (half-residue in the pole $s' = s$), and the real part is the principal value of the integral (15). The real part, $\mathrm{Re}\, B(s)$, does not contain the $\pi\pi$-threshold singularity; this singularity is defined by the phase space factor in the imaginary part, $\rho_{\pi\pi}(s)$. So we may re-write the amplitude $A(s)$ in the form

$$A(s) \;=\; \frac{K(s)}{1-i\rho_{\pi\pi}(s)K(s)}\;, \tag{16}$$

where in the right-hand half-plane $s > 0$ the K-matrix block

$$K(s) \;=\; \frac{N(s)}{1-\mathrm{Re}\; B(s)}\;, \tag{17}$$

may have the pole singularities only, and in the left-hand one, $s \leq 0$, it contains a set of left-hand singularities. By singling out the left-hand side singularities in the explicit form, one can write the K-matrix block as follows:

$$K(s) \;=\; \sum_i \frac{g_i^2}{m_i^2-s} + f(s)\;, \tag{18}$$

where the pole positions, m_i^2, are given by the equalities:

$$[1-\mathrm{Re}\; B(s)]_{s=m_i^2} \;=\; 0\;, \tag{19}$$

and $f(s)$ contains all left-hand singularities:

$$f(s) \;=\; \frac{N(s)}{1-\mathrm{Re}\; B(s)} - \sum_i \frac{g_i^2}{m_i^2-s} \;=\; \int\limits_{s_L}^{-\infty} \frac{ds'}{\pi}\;\frac{\mathrm{disc}\; f(s')}{s'-s}\;. \tag{20}$$

The magnitude s_L defines the location of the closest left-hand singularity; for the considered $\pi\pi$-scattering amplitude, $s_L = 0$.

In the physical region, a suitable approximation for the amplitude is given by substituting the spectral integral (20) with the sum:

$$\int\limits_{s_L}^{-\infty} \frac{ds'}{\pi} \, \frac{\mathrm{disc}\ f(s')}{s'-s} \ \longrightarrow \ \sum_n \frac{f_n}{s+s_n} \ , \tag{21}$$

where $s_n > -s_L$. In the multichannel analyses [8, 9], the approximation had been used, when the left-hand cut in the K-matrix terms K_{ab} was fitted to the one-pole term as follows:

$$f_{ab}(s) \ \to \ \frac{f_{ab}}{s+s_0} \ . \tag{22}$$

The parameter s_0 in different variants of the fit [8] appeared in the interval $0.5 \lesssim s_0 \lesssim 1.5\,\mathrm{GeV}^2$, that points to a large contribution of the t- and u-channel f_2, ρ and σ exchanges. The use of the two-pole approximation for the multichannel K-matrix deteriorates the convergence of the fitting procedure, for the available experimental data are insufficient to fix unambigously a large number of the left-hand-cut parameters.

More fruitful for the reconstruction of analytical structure of the amplitude near $s \sim 0$ is the fitting to the 00^{++} wave in the region $s < 1000$ MeV, when one may restrict oneself by the one-channel approximation. In Section 3.8, we present more detailed narration of the study of analytical structure of the amplitude at the region $s \sim 0 - 4m_\pi^2$, with the restoration of the left-hand singularities obeying equations (20) and (21); this topic is related to the light σ-meson problem.

3.1.3 Three-meson production in the reactions of the $p\bar{p}$ and $n\bar{p}$ annihilation

The K-matrix representation of the amplitude may be applied to the description of the production of resonances in the three or more particle production. The uniformity of the amplitude representation is important in the combined analysis of the two-particle, like $\pi\pi \to \pi\pi, K\bar{K}$, and multiparticle, like $p\bar{p} \to \pi\pi\pi, \pi\eta\eta, \pi K\bar{K}$, reactions. The K-matrix approach to multiparticle processes is based on the fact that the denominator of the K-matrix two-particle amplitude (12), $[1 - \hat{\rho}\hat{K}]^{-1}$, describes pair interactions of mesons in the final state as well.

Let us clarify this statement using as an example the amplitude of the $p\bar{p}$ annihilation from the ${}^1S_0$ level: $p\bar{p}({}^1S_0) \to three\,mesons$. Let the produced mesons be labelled by the indices 1,2,3; then the production amplitude for the resonance with the spin $J = 0$ in the channel (1,2) is as follows:

$$A_3(s_{12}) = K_3^{(prompt)}(s_{12})[1 - i\rho_{12}\widehat{K}_{12}(s_{12})]^{-1}, \tag{23}$$

where the matrix factor $[1 - i\hat{\rho}_{12}\widehat{K}_{12}(s_{12})]^{-1}$ depends on the invariant energy squared of the mesons 1 and 2 and it coincides with matrix factor of the two-particle amplitude

(12). The factor $\widehat{K}_3^{(prompt)}(s_{12})$ stands for the prompt production of particles 1,2 and resonances in this channel:

$$\Big(K_3^{(prompt)}(s_{12})\Big)_{ab} = \sum_n \frac{\Lambda_a^{(n)} g_b^{(n)}}{\mu_n^2 - s_{12}} + \varphi_{ab}(s_{12}) \ , \tag{24}$$

where $\Lambda_a^{(n)}$ and φ_{ab} are the parameters of the prompt-production amplitude, and $g_b^{(n)}$ and μ_n are defined by the two-meson scattering amplitude, see (12).

It is also appropriate to mention that the description of the two-particle interactions by using the K-matrix factor $(1-\hat{\rho}\hat{K})^{-1}$ is nothing else than a generalization of the well-known Watson–Migdal formula used for the two-nucleon interactions at low energies in nuclear reactions with multiple production of nucleons [47].

The whole amplitude for the production of the $(J = 0)$-resonances is defined by the sum of contributions from all channels:

$$A_3(s_{12}) + A_2(s_{13}) + A_1(s_{23}) \tag{25}$$

To account for resonances with the nonzero spin J one needs to substitute in (23):

$$A_3(s_{12}) \to \sum_J A_3^{(J)}(s_{12}) X^{(J)}_{\mu_1\mu_2\ldots\mu_J}(k_{12}^{\perp}) X^{(J)}_{\mu_1\mu_2\ldots\mu_J}(k_3^{\perp}), \tag{26}$$

where the K-matrix amplitude $A_3^{(J)}(s_{12})$ is determined by the expression similar to (23), and $X^{(J)}_{\mu_1\mu_2\ldots\mu_J}$ stands for meson states with the angular momentum J. The angular-momentum operators depend on the perpendicular components of meson relative momenta: $k_{12}^{\perp}$ and $k_3^{\perp}$. Here $k_{12}^{\perp}$ is the component of relative momentum of particles 1 and 2, $k_{12} = (k_1 - k_2)/2$, which is orthogonal to the total momentum of particles 1 and 2, $p_{12} = (k_1 + k_2)$, namely, $(k_{12}^{\perp} p_{12}) = 0$; likewise, $(k_3^{\perp} p) = 0$, where $p = k_1 + k_2 + k_3$.

For the lowest angular momenta, the operators $X^{(J)}_{\mu_1\mu_2\ldots\mu_J}$ can be easily written; for example, for $J = 1, 2$ we have, up to the normalization factor, $X^{(1)}_{\mu}(k^{\perp}) \sim k^{\perp}_{\mu}$ and $X^{(2)}_{\mu_1\mu_2}(k^{\perp}) \sim (k^{\perp}_{\mu_1} k^{\perp}_{\mu_2} - \frac{1}{3} k^{\perp 2} g^{\perp}_{\mu_1\mu_2})$, where $g^{\perp}_{\mu_1\mu_2}$ is the metric tensor in the space orthogonal to the total momentum. The construction of operators for arbitrary J may be found in [48].

The covariant operators $X^{(J)}_{\mu_1\mu_2\ldots\mu_J}$ are determined in the four-momentum space; this is a relativistic generalization of the 3-dimensional angular-momentum operators of Zemach [49]. The use of the 4-dimentional operators is suitable for the analysis of multiparticle final states, for in this case one does not need numerous Lorentz boosts, which are necessary in the Zemach technique or by using spherical functions.

The amplitude expansion with respect to the states with different angular momenta by using relativistic covariant operators has been carried out for all the reactions $p\bar{p} \to$ *three mesons*, in the analysis of which the PNPI group took part [2, 3, 4, 5, 6, 8]. Such an expansion, apart from being simple and compact, as was mentioned above, has an advantage of taking correct account of kinematical factors, which are significant for the

reconstruction of the correct behaviour of the threshold singularities of multiparticle amplitude. In the other orbital-moment decomposition techniques this is a subject of a special care; in particular, in [50] a special method was suggested to take account of kinematical factors by using the expansion with respect to spherical functions.

In the paper [48], the operators are also constructed for spins and total angular momenta in case of fermion and photon systems, which are used for the analysis of the reactions $p\bar{p} \to mesons$ and $\gamma\gamma \to mesons$.

The formula (23) serves us for singling out the pole singularities of the amplitude $p\bar{p}(^1S_0) \to three\, mesons$, which are the leading ones. The next-to-leading logarithmic singularities are related to the rescattering of mesons produced by the decaying resonances (that is, triangle-diagram singularities [34]). The analysis performed in [2, 4] showed that in the reactions $p\bar{p}(\text{at rest}) \to \pi^0\pi^0\pi^0$, $\pi^0\pi^0\eta$, $\pi^0\eta\eta$, to determine parameters of a resonance produced in the two-meson channels one may not take into consideration explicitly the triangle diagram singularities — it is important to account only for the complex-valuedness of the prompt production amplitude, that is due to final-state interactions (that is, the complexity of parameters $\Lambda_a^{(n)}$ and φ_{ab} in (24)). Note that it is not a universal rule for the meson production processes in the $p\bar{p}$ annihilation — for example, in the reaction $p\bar{p} \to \eta\pi^+\pi^-\pi^+\pi^-$ [37], the explicit form of the triangle singularity is important.

A complete account for unitarity and analyticity in the three-meson production amplitude is related to the consideration of a full set of meson interactions in the final state. In the reactions $p\bar{p}(\text{at rest}) \to \pi\pi\pi$, $\pi\pi\eta$, $\pi\eta\eta$, $\pi K\bar{K}$, the connected system of the dispersion-relation N/D equations, with all pair-meson equations accounted for, has been written in [51]. The three-meson production amplitudes being related to each other by the N/D equations leave less freedom for the fitting than formula (23) and, in principle, they provide more information about meson–meson amplitudes. However, the fitting on the basis of the N/D equations is much more complicated procedure than the K-matrix analysis.

3.1.4 Peripheral two-meson production in meson–nucleon collisions at high energies

The two-meson production reactions $\pi p \to \pi\pi n$, $K\bar{K}n$, $\eta\eta n$, $\eta\eta' n$ at high energies and small momentum transfers to the nucleon, t, provide us with a direct information about the amplitudes $\pi\pi \to \pi\pi$, $K\bar{K}$, $\eta\eta$, $\eta\eta'$, for at $|t| < 0.2\,(\text{GeV/c})^2$ the reggeized π exchange dominates the production reactions. At larger $|t|$, the change of the regime occurs: at $|t| \gtrsim 0.2\,(\text{GeV/c})^2$ a significant contribution of other reggeons become plausible (a_1-exchange, daughter π- and a_1-exchanges). Despite a vague knowledge of the exchange structure, the study of the two-meson production processes at $|t| \sim 0.5 - 1.5\,(\text{GeV/c})^2$ looks rather attractive, for at such momentum transfers the broad resonance vanishes, so the production of the $f_0(980)$ and $f_0(1300)$ appears practically without background, that is important for finding parameters of these resonances.

The amplitude of the peripheral production of two S-wave mesons reads:

$$(\bar{\psi}_N \hat{0}_R \psi_N) R(s_{\pi N}, t) \widehat{K}_{\pi R(t)} \left[1 - \hat{\rho}\widehat{K}\right]^{-1} \ , \tag{27}$$

where the factor $(\bar{\psi}_N \hat{0}_R \psi_N)$ stands for the reggeon–nucleon vertex, and $\hat{0}_R$ is the spin operator; $R(s_{\pi N}, t)$ is the reggeon propagator depending on the total energy squared of colliding particles, $s_{\pi N}$, and momentum transfer squared t, and the factor $\widehat{K}_{\pi R(t)}[1 - i\hat{\rho}\widehat{K}]^{-1}$ is related to the block of the two-meson production — one may find the detailed description of the amplitude (27) in [8, 52].

The factor $\widehat{K}_{\pi R(t)}[1 - i\hat{\rho}\widehat{K}]^{-1}$ describes the transitions $\pi R(t) \to \pi\pi$, $K\bar{K}$, $\eta\eta$, $\eta\eta'$: the block $\widehat{K}_{\pi R(t)}$ is associated with the prompt meson production , and $[1 - i\hat{\rho}\widehat{K}]^{-1}$ is a standard factor for meson rescattrings, see (12). The prompt-production block is parametrized as follows:

$$\left(\widehat{K}_{\pi R(t)}\right)_{\pi R,b} \ = \ \sum_n \frac{G^{(n)}_{\pi R}(t) g^{(n)}_b}{\mu_n^2 - s} + f_{\pi R,b}(t,s) \ , \tag{28}$$

where $G^{(n)}_{\pi R}(t)$ is the f_0 production vertex, and $f_{\pi R,b}$ stands for the background production of mesons, while the parameters $g^{(n)}_b$ and μ_n are the same as in the transition amplitude $\pi\pi \to \pi\pi$, $K\bar{K}$, $\eta\eta$, $\eta\eta'$, see (12).

At the early stage of the analysis of the S-wave two-pion production, $\pi^- p \to (\pi\pi)_S\, n$, the mechanism of the reggeized-π exchange was suggested both at small and moderately large $|t|$ [53]. The change of the regime at $|t| \sim 0.2 - 0.4\,(\mathrm{GeV/c})^2$ has been described by including the effective πP-exchange (P is the pomeron): the amplitude of the πP-exchange has another sign than the π-exchange, thus leading to the amplitude zero and, correspondingly, to a zero in the t-distribution at $|t| \sim 0.3\,(\mathrm{GeV/c})^2$, where the regime changes. The filling-in of the dips in the t-distributions at $|t| \sim 0.3\,(\mathrm{GeV/c})^2$ can appear due to exchanges of other reggeons, namely, reggeized a_1-exchange and contributions from the daughter trajectories, $\pi_{(daughter)}$ and $a_{1(daughter)}$. Practically, all these terms do not interfere in the reaction $\pi^- p \to (\pi\pi)_S\, n$: the π- and a_1-exchanges do not interfere due to different spin structures in reggeon–nucleon vertices, ($\hat{0}_\pi \sim \boldsymbol{\sigma}_\perp$ and $\hat{0}_{a_1} \sim \boldsymbol{\sigma}_\parallel$, where $\boldsymbol{\sigma}_\perp$ and $\boldsymbol{\sigma}_\parallel$ are the transverse and longitudinal components of the Pauli matrix operating in the spin space of the nucleon). At the same time the contributions of leading and daughter trajectories do not interfere practically due to a phase shift in reggeon propagators (for example, the propagator of the leading π-trajectory may be considered, with a good accuracy, as real magnitude, while the propagator of the $\pi_{(daughter)}$-trajectory is nearly imaginary), see [52] for more detail.

The a_1 exchange for the reaction $\pi p \to (\pi\pi)_S\, n$ was considered in [10, 54]. In [10], the calculations of the $\pi\pi$ spectra were performed both with the a_1 exchange and within an effective π exchange. As a result, it occurred that the a_1 exchange affects weakly the parameters of the $f_0(980)$ and $f_0(1300)$: the matter is that the $\pi\pi$ spectra measured by GAMS group [12] were averaged over large t-intervals, thence the details of the t-distributions are not significant for fixing resonance parameters.

New data on the production of the $\pi\pi$ system at $|t| \leq 1.5\,(\mathrm{GeV/c})^2$ [18] gave rise to the discussion about the role of the t exchange in the definition of parameters of the $f_0(980)$ and $f_0(1300)$. The data of the E852 Collaboration obtained at lower energies ($p_{lab} = 18\,\mathrm{GeV/c}$) as compared to the GAMS energy ($p_{lab} = 38\,\mathrm{GeV/c}$) point definitely to the fact that the description of the peripheral pion production $\pi^- p \to (\pi\pi)_S n$ in terms of the leading t exchanges, π and a_1, is not complete: the alteration of spectra with energy in the region $|t| \sim 0.3 - 0.4\,(\mathrm{GeV/c})^2$ and $M_{\pi\pi} \sim 1300\,\mathrm{MeV}$ proved a considerable weight of daughter trajectories: $\pi_{(daughter)}$ and/or $a_{1(daughter)}$.

Combined analysis of the $(\pi\pi)_S$ spectra by GAMS [12] and E852 [18] at $|t| \leq 1.5\,(\mathrm{GeV/c})^2$ has been performed in [52]. The analysis [52] showed that, though the data do not allow us to find out the t exchange mechanism unambigously, this circumstance affects weakly the definition of parameters of the produced $f_0(980)$ and $f_0(1300)$ resonances: in all variants of the fit (including various combinations of the $\pi_{(leading)}$, $a_{1(leading)}$, $\pi_{(daughter)}$, $a_{1(daughter)}$ exchanges, the consideration of the effective πP and $a_1 P$ exchanges at $|t| \gtrsim 0.2\,(\mathrm{GeV/c})^2$, with P being the pomeron, or the Orear mechanism [55]) the parameters of $f_0(980)$ and $f_0(1300)$ are almost the same. This circumstance allows us to restrain ourselves in the K-matris fit [8] by the two variants of the t-channel mechanism, namely, $\pi_{(leading)}$, $a_{1(leading)}$, $\pi_{(daughter)}$ or $\pi_{(leading)}$, $a_{1(leading)}$, $a_{1(daughter)}$.

An opposite statement, according to which the choice of the t-exchange mechanism influences signficantly the definition of the parameters of $f_0(980)$ and $f_0(1300)$, was claimed in [56] (though without performing the fitting to resonance parameters). However, the analysis [52] does not confirm the statements of [56].

3.2 Classification of scalar bare states

The systematics of scalar bare states has been carried out in [57], where bare K-mesons were found which are needed to fix two quark-antiquark nonets, $1^3P_0 q\bar{q}$ and $2^3P_0 q\bar{q}$. The $q\bar{q}$ nonet contains two scalar–isoscalar states, $f_0^{bare}(1)$ and $f_0^{bare}(2)$, scalar–isovector meson a_0^{bare} and scalar kaon K_0^{bare}. The decay couplings to pseudoscalar mesons for these four states,

$$\begin{aligned} & f_0^{bare}(1),\ f_0^{bare}(2) \ \to\ \pi\pi, K\bar{K}, \eta\eta, \eta\eta' \ , \\ & a_0^{bare} \ \to\ \pi\eta,\ K\bar{K} \ , \\ & K_0^{bare} \ \to\ \pi K,\ \eta K \ , \end{aligned} \tag{29}$$

are determined, in the leading-order terms of the $1/N$-expansion [58], by three parameters only. They are the common decay coupling g, parameter λ for the probability to produce strange quarks in the decay process (in the limit of a precise $SU(3)_{flavour}$ symmetry we have $\lambda = 1$) and mixing angle for $s\bar{s}$ and $n\bar{n} = (u\bar{u} + d\bar{d})/\sqrt{2}$ components in the f_0-mesons, $\psi_{flavour}(f_0) = n\bar{n}\cos\varphi + s\bar{s}\sin\varphi_i$. For the nonet partners, $\varphi[f_0^{bare}(1)] - \varphi[f_0^{bare}(2)] = 90^\circ$.

The rigid constraints on the decay couplings of bare states (29) are imposed by the quark-combinatorics relations. The rules of quark combinatorics were first suggested for the high-energy hadron production [59] and then extended for hadronic J/Ψ decays [60]. The quark-combinatorics relations were used for the decay couplings of the scalar-isoscalar states in the analysis of the quark-gluonium content of resonances in [61] and later on in the K-matrix analyses [8, 9, 10, 11, 20, 57].

These constraints being imposed on the decay couplings (29) provide us with an opportunity to fix unambigously the states belonging to the basic nonet [57], also see [8, 9]:

$$\begin{aligned} 1^3P_0q\bar{q}\ : \qquad & f_0^{bare}(700\pm 100),\ f_0^{bare}(1220\pm 40)\ , \\ & a_0^{bare}(960\pm 30),\ K_0^{bare}\left(1220^{+50}_{-150}\right)\ , \end{aligned} \tag{30}$$

as well as the mixing angle for $f_0^{bare}(700)$ and $f_0^{bare}(1220)$,

$$\begin{aligned} \varphi[f_0^{bare}(700)] &= -70^\circ\pm 10^\circ\ , \\ \varphi[f_0^{bare}(1220)] &= 20^\circ\pm 10^\circ\ , \end{aligned} \tag{31}$$

To establish the nonet of the first radial excitation, $2^3P_0q\bar{q}$, is more complicated task. The K-matrix analysis gives us two scalar-isoscalar bare states at 1200–1650 MeV, $f_0^{bare}(1230\pm 40)$ and $f_0^{bare}(1580\pm 40)$, whose decay couplings (29) obey the relations appropriate to the glueball. The matter is that the relations between couplings for the glueball decay, $glueball\to\pi\pi, K\bar{K}, \eta\eta, \eta\eta'$, and the decay couplings of the quark-antiquark flavour singlet, $(q\bar{q})_{singlet}\to\pi\pi, K\bar{K}, \eta\eta, \eta\eta'$, are almost the same (they are exactly the same in the limit $\lambda = 1$). Because of that, it is impossible, by using hadronic decay couplings only, to distinguish between the glueball and flavour singlet.

Systematics of bare $q\bar{q}$-states on the (n, M^2)-plane helps us to resolve the dilemma which one of these states is the glueball. This systematics (which is discussed in more detail in Section 3.8) definitely tells us that the state $f_0^{bare}(1580\pm 40)$ not being on the $q\bar{q}$-trajectory is an extra one, so furthermore we accept that this state is the glueball. Indeed,

$$0^{++}\ \text{glueball}: \quad f_0^{bare}(1580\pm 40)\ . \tag{32}$$

Lattice calculations [62] agree with this statement: gluodynamical glueball should be in the mass range 1550–1750 MeV.

Having accepted the $f_0^{bare}(1580\pm 40)$ to be non-$q\bar{q}$-state, we construct the nonet $2^3P_0q\bar{q}$ in a unique way:

$$\begin{aligned} 2^3P_0q\bar{q}\ : \qquad & f_0^{bare}(1230\pm 40),\ f_0^{bare}(1800\pm 30)\ , \\ & a_0^{bare}(1650\pm 50),\ K_0^{bare}\left(1885^{+50}_{-100}\right)\ . \end{aligned} \tag{33}$$

The kaonic bare states were defined in the K-matrix analysis of the πK-spectrum performed in [57] on the basis of data [63]. This analysis provided us with a few solutions. In (30) and (33) the values of $K_0^{bare}(1220^{+50}_{-150})$ and $K_0^{bare}(1885^{+50}_{-100})$ were

used, which were the average ones for these solutions: a large error in the determination of masses of bare states resulted from the variaty of mass values coming from different solutions.

After switching on the decay channels, the bare states (30), (32), (33) turn into real resonances. For scalar–isoscalar states we have, after the decay onset, the transformation as follows:

$$\begin{aligned} f_0^{bare}(700 \pm 100) &\longrightarrow f_0(980) \ , \\ f_0^{bare}(1220 \pm 40) &\longrightarrow f_0(1300) \ , \\ f_0^{bare}(1230 \pm 40) &\longrightarrow f_0(1500) \ , \\ f_0^{bare}(1580 \pm 40) &\longrightarrow f_0(1200-1600) \ , \\ f_0^{bare}(1800 \pm 40) &\longrightarrow f_0(1750) \ . \end{aligned} \tag{34}$$

This evolution of states is illustrated by Fig. 5, where the shift of amplitude poles into comlex plane is shown depending on gradual onset of the decay channels. Technically, it is not difficult to switch on/off the decay channels for the K-matrix amplitude: one should substitute in the K-matrix elements (11):

$$g_a^{(n)} \ \rightarrow \ \xi_n(x) g_a^{(n)} \ , \qquad f_{ab} \ \rightarrow \ \xi_f(x) f_{ab} \ , \tag{35}$$

where the parameter-functions for switching on/off the decay channels, $\xi_n(x)$ and $\xi_f(x)$, satisfy the following constraints: $\xi_n(0) = \xi_f(0) = 0$ and $\xi_n(1) = \xi_f(1) = 1$, and x varies in the interval $0 \leq x \leq 1$. Then, at $x = 0$, the amplitude $\widehat{A}$ turns into the K-matrix, $\widehat{A}(x \rightarrow 0) \rightarrow \widehat{K}$, and the amplitude poles occur on the real axis, that corresponds to the stable f_0^{bare}-states. At $x = 1$, we deal with real resonance; varying x from $x = 0$ to $x = 1$ we observe the shift of poles into the complex M-plane.

The x-dependence of $\xi_n(x)$ and $\xi_f(x)$ is governed by the dynamics of the state mixing, and the K-matrix solution does not clear up this dynamics. In [64], the mixing has been modelled within the two-component approach for the decay processes, when the resonance widths are due to the transitions $f_0 \rightarrow q\bar{q}$ and $f_0 \rightarrow gg$. This model proved that just the glueball accumulated the widths of neighbouring $q\bar{q}$ states. The dominant accumulation of widths by the glueball occurs by virtue of two reasons. First, mutual transitions $q\bar{q}$-*mesons* $\leftrightarrow$ *glueball* are not suppressed within the $1/N$ expansion rules, e.g. see [11]. Second, the orthogonality of the $q\bar{q}$-states suppresses direct mixing of the $q\bar{q}$-mesons.

3.3 Ovelapping f_0-resonances in the region 1200–1700 MeV: the accumulation of widths of quark-antiquark states by the glueball

The formation of the broad state is not an accidental phenomenon. The broad state appeared as a result of mixture of resonances, due to the transitions $f_0(1) \rightarrow$ *real mesons* $\rightarrow$

$f_0(2)$. Such transitions in case of overlapping resonances, result in a specific phenomenon: when several resonances with common decay channels overlap, one of them accumulates the widths of neighbouring resonances. So a broad resonance appears together with several narrow ones.

Initially, the effect of accumulation of widths had been discussed in nuclear physics [65, 66, 67]. Concerning the scalar 00^{++}-mesons, the accumulation of widths by one of overlapping resonances was observed in [20, 36, 68]. In [68, 69], the following scheme has been suggested: the broad state $f_0(1200-1600)$ is the glueball descendant; this state was formed because of the glueball mixing with neighbouring $q\bar{q}$-states, that was accompanied by the accumulation of widths of neighbouring states by the glueball descendant. As a result, comparatively narrow states $f_0(1300)$, $f_0(1500)$, $f_0(1750)$ have had considerable admixtures of the glueball component, while the broad state got a large $q\bar{q}$-component. The quark-antiquark component in the glueball should be close to the flavour singlet, namely [21]:

$$(q\bar{q})_{glueball} = (u\bar{u} + d\bar{d} + \sqrt{\lambda}s\bar{s})/\sqrt{2+\lambda}, \tag{36}$$

where the parameter λ is nearly the same as that in the decay processes, $\lambda \simeq 0.5 - 0.8$.

In meson physics, the accumulation of widths can play a decisive role for the destiny of exotic states which are beyond the $q\bar{q}$ systematics. Indeed, the exotic state, after appearing in a set of $q\bar{q}$-states, creates a group of overlapping resonances. If the transition of the exotic state into $q\bar{q}$-state is not suppressed (as in case of the glueball, where, according to the $1/N$-expansion rules [58], the transition $glueball \to q\bar{q}\text{-}meson$ is allowed in the leading-order terms [11, 70]), then just the exotic meson has an advantage to accumulate the widths: the wave functions of neighbouring $q\bar{q}$-states are orthogonal to each other but not to the exotic state. Therefore, the existence of the broad state together with comparatively narrow ones must serve as a signature of exotics in this mass region [71].

The broad state may play rather constructive role in the formation of the confinement barrier. The broad state, after accumulating the widths of resonances–neighbours in the mass scale, plays the role of a locking state. The evaluation of radii of the broad state $f_0(1200-1600)$ and two narrow neighbouring ones, $f_0(980)$ and $f_0(1300)$, which was performed in [10, 72], tells us that the radius of the broad state is considerably larger than the radii of $f_0(980)$ and $f_0(1300)$: this fact agrees well with the assumption that $f_0(1200-1600)$ plays the role of a locking state for its resonance-neighbours. Recent measurement of the t-distributions in the reaction $\pi^- n \to (\pi\pi)_S\, n$ [18] confirmed relatively large magnitude of the broad state radius: with the increase of $|t|$ (momentum square transferred to the resonance), the broad state vanishes much faster than $f_0(980)$ and $f_0(1300)$.

Table 4: Coupling constants squared (in GeV^2) of scalar–isoscalar resonances decaying to the hadronic channels $\pi\pi$, $K\bar{K}$, $\eta\eta$, $\eta\eta'$ and $\pi\pi\pi\pi$ for different K-matrix solutions.

Pole position	$\pi\pi$	$K\bar{K}$	$\eta\eta$	$\eta\eta'$	$\pi\pi\pi\pi$	Solution
$f_0(980)$						
$1031 - i32$	0.056	0.130	0.067	–	0.004	I
$1020 - i35$	0.054	0.117	0.139	–	0.004	II
$f_0(1300)$						
$1306 - i147$	0.036	0.009	0.006	0.004	0.093	I
$1325 - i170$	0.053	0.003	0.007	0.013	0.226	II
$f_0(1500)$						
$1489 - i51$	0.014	0.006	0.003	0.001	0.038	I
$1490 - i60$	0.018	0.007	0.003	0.003	0.076	II
$f_0(1750)$						
$1732 - i72$	0.013	0.062	0.002	0.032	0.002	I
$1740 - i160$	0.089	0.002	0.009	0.035	0.168	II
$f_0(1200 - 1600)$						
$1480 - i1000$	0.364	0.265	0.150	0.052	0.524	I
$1450 - i800$	0.179	0.204	0.046	0.005	0.686	II

3.4 Evolution of couplings of the 00^{++}-states to channels $\pi\pi$, $\pi\pi\pi\pi$, $K\bar{K}$, $\eta\eta$ $\eta\eta'$ with the onset of decay processes

The K-matrix analysis does not allow one to determine partial widths of the f_0-resonances directly. To find out partial widths for the decays $f_0 \to \pi\pi$, $\pi\pi\pi\pi$, $K\bar{K}$, $\eta\eta$, $\eta\eta'$ it is necessary to calculate the residues of the amplitude poles corresponding to resonances. Near the resonance, the transition amplitude $a \to b$ (indices a and b stand for the resonance channels $\pi\pi$, $K\bar{K}$, $\eta\eta$, $\eta\eta'$, $\pi\pi\pi\pi$) takes the form:

$$A_{ab} \;\simeq\; \frac{g_a^{(n)} g_b^{(n)}}{\mu_n^2 - s}\; e^{i(\theta_a^{(n)} + \theta_b^{(n)})} + B_{ab}\ . \tag{37}$$

The pole position defines the mass and width of the resonance $\mu_n = M_n - i(\Gamma_n/2)$, and the real-valued coupling constants to channels, $g_a^{(n)}$ and $g_b^{(n)}$, allow us to find partial widths of resonances. Factorized residues are complex-valued magnitudes, their complexity is determined in (37) by the phases $\theta_a^{(n)}$ and $\theta_b^{(n)}$; in (37), a smooth, non-pole, term B_{ab} is also written.

On the basis of the results of the K-matrix fit [8], the decay coupling constants $g_a^{(n)}$ were calculated for $f_0(980)$, $f_0(1300)$, $f_0(1500)$, $f_0(1750)$ and the broad state $f_0(1200 - 1600)$, and the comparison was done for the obtained values with corresponding couplings of bare states, which are predecessors of the resonances under discussion.

The values of couplings calculated in [8] are shown in Table 4. The comparison reveals a significant difference between the decay couplings for bare states and their

descendant–resonances. This undoubtedly proves a strong effect of the mixing of $q\bar{q}$-states with the glueball: the real resonance is a mixture of these states.

Figure 6 demonstrates the evolution of coupling constants at the onset of the decay channels: following [73], relative changes of coupling constants are shown for $f_0(980)$, $f_0(1300)$, $f_0(1500)$ and $f_0(1750)$ after switching on/off the decay channels (recall that the value $x = 0$ corresponds to the amplitude poles on the real axis and the value $x = 1$ stands for the resonance observed experimentally).

Let us bring our attention to a rapid increase of the coupling constant $f_0 \to K\bar{K}$ at the trajectory $f_0^{bare}(700) - f_0(980)$ in the region $x \sim 0.8 - 1.0$, where $\gamma^2(x = 1.0) - \gamma^2(x = 0.8) \simeq 0.2$, see Fig. 6a. Actually this increase is the upper limit of the possible admixure of the long-range $K\bar{K}$ component in the $f_0(980)$: it cannot be greater than 20%.

3.5 Evaluation of the glueball component in the resonances $f_0(980)$, $f_0(1300)$, $f_0(1500)$, $f_0(1750)$ and broad state $f_0(1200-1600)$ based on the analysis of hadronic-decay channels

The evolution of couplings observed in the transition from bare states to real resonances is due to the mixture of the $q\bar{q}$-states with the glueball that is a consequence of the transitions $f_0(1) \to \textit{real mesons} \to f_0(2)$. One can evaluate the quark-antiquark and glueball components in $f_0(980)$, $f_0(1300)$, $f_0(1500)$, $f_0(1750)$ and $f_0(1200-1600)$ using the rules of quark combinatorics for the decay couplings.

In the leading-order terms of the $1/N$-expansion the vertices of hadronic decays of the resonances are defined by planar diagrams, the examples of the planar diagram for the decay of $q\bar{q}$-state and the glueball into two mesons are presented in Fig. 7a,b, respectively. In the course of the $q\bar{q}$-state decay, the gluons produce a new $q\bar{q}$-pair; in the glueball decay, a subsequent production of two pairs occurs.

For the decay couplings squared for $f_0 \to \pi\pi, K\bar{K}, \eta\eta, \eta\eta'$, the quark-combinatorics rules, in case when the f_0 state is the mixture of the quarkonium and gluonium components, give us [8, 73]:

$$
\begin{aligned}
g^2_{\pi\pi} &= \frac{3}{2}\left(\frac{g}{\sqrt{2}}\cos\varphi + \frac{G}{\sqrt{2+\lambda}}\right)^2, \\
g^2_{K\bar{K}} &= 2\left(\frac{g}{2}(\sin\varphi + \sqrt{\frac{\lambda}{2}}\cos\varphi) + G\sqrt{\frac{\lambda}{2+\lambda}}\right)^2, \\
g^2_{\eta\eta} &= \frac{1}{2}\left(g(\frac{\cos^2\Theta}{\sqrt{2}}\cos\varphi + \sqrt{\lambda}\sin\varphi\sin^2\Theta) + \frac{G}{\sqrt{2+\lambda}}(\cos^2\Theta + \lambda\sin^2\Theta)\right)^2, \\
g^2_{\eta\eta'} &= \sin^2\Theta\cos^2\Theta\left(g(\frac{1}{\sqrt{2}}\cos\varphi - \sqrt{\lambda}\sin\varphi) + G\frac{1-\lambda}{\sqrt{2+\lambda}}\right)^2.
\end{aligned}
\tag{38}
$$

The terms proportional to g stand for the transitions $q\bar{q} \to$ *two mesons*, while those with G respond to transitions *glueball* $\to$ *two mesons*. Accordingly, g^2 and G^2 are proportional to the probability to find in the considered f_0-meson the quark-antiquark and glueball componets. Recall that the angle φ stands for the content of the $q\bar{q}$-component in the decaying state, $q\bar{q} = \cos\varphi\, n\bar{n} + \sin\varphi\, s\bar{s}$, and the angle Θ for the contents of η and η' mesons: $\eta = \cos\Theta\, n\bar{n} - \sin\Theta\, s\bar{s}$ and $\eta' = \sin\Theta\, n\bar{n} + \cos\Theta\, s\bar{s}$; we use $\Theta = 38^\circ$ [74].

One may believe that the decay of the glueball is going in two steps: initially, one $q\bar{q}$ pair is produced, then with the production of the next $q\bar{q}$ pair a fusion of quarks into mesons occurs. Therefore, at the intermediate stage of the f_0 decay, we deal with a mean quantity of the quark-antiquark component, $\langle q\bar{q}\rangle$, which later on turns into hadrons. The equation (38), under the condition $G = 0$, defines the content of this intermediate state $\langle q\bar{q}\rangle = n\bar{n}\cos\langle\varphi\rangle + s\bar{s}\sin\langle\varphi\rangle$.

As was said above, the K-matrix analysis [8] gave us two Solutions, **I** and **II**, which differ mainly by the parameters of the resonance $f_0(1750)$. Fitting to the decay couplings squared for these Solutions leads to the values of $\langle\varphi\rangle$ as follows:

Solution **I**:

$$\begin{aligned}
f_0(980): &\quad \langle\varphi\rangle \simeq -68^\circ\,, &&\lambda \simeq 0.5 - 1.0\,, \\
f_0(1300): &\quad \langle\varphi\rangle \simeq (-3^\circ) - 4^\circ\,, &&\lambda \simeq 0.5 - 0.9\,, \\
\text{Broad state } f_0(1200-1600): &\quad \langle\varphi\rangle \simeq 27^\circ\,, &&\lambda \simeq 0.54\,, \\
f_0(1500): &\quad \langle\varphi\rangle \simeq 12^\circ - 19^\circ\,, &&\lambda \simeq 0.5 - 1.0\,, \\
f_0(1750): &\quad \langle\varphi\rangle \simeq -72^\circ\,, &&\lambda \simeq 0.5 - 0.7\,,
\end{aligned} \tag{39}$$

Solution **II**:

$$\begin{aligned}
f_0(980): &\quad \langle\varphi\rangle \simeq -67^\circ\,, &&\lambda \simeq 0.6 - 1.0\,, \\
f_0(1300): &\quad \langle\varphi\rangle \simeq (-16^\circ) - (-13^\circ)\,, &&\lambda \simeq 0.5 - 0.6\,, \\
\text{Broad state } f_0(1200-1600): &\quad \langle\varphi\rangle \simeq 33^\circ\,, &&\lambda \simeq 0.85\,, \\
f_0(1500): &\quad \langle\varphi\rangle \simeq 2^\circ - 11^\circ\,, &&\lambda \simeq 0.6 - 1.0\,, \\
f_0(1750): &\quad \langle\varphi\rangle \simeq -18^\circ\,, &&\lambda \simeq 0.5\,.
\end{aligned} \tag{40}$$

In both Solutions, the average values of mixing angle for $f_0(980)$ coincide with one another, with a good accuracy. Still, one should inderline that equations (38) allow us to get one more magnitude for the mixing angle of the $f_0(980)$, namely, $\langle\varphi[f_0(980)]\rangle \simeq 40^\circ$. The fact that the decay constants for $f_0(980) \to \pi\pi$ and $f_0(980) \to K\bar{K}$ accept the

solution with $\langle\varphi[f_0(980)]\rangle \simeq 40^\circ$ was underlined in [75]. However, this value of mixing angle does not suit the classification of bare states provided by the K-matrix solutions. Indeed, the $f_0(980)$ is the descendant of the bare state $f_0^{bare}(700\pm100)$ which is close to the flavour octet. The evolution of coupling constants (see Fig. 6) tells us that $f_0(980)$ by its content remains close to its predecessor, $f_0^{bare}(700 \pm 100)$. Because of that, in Eqs. (39) and (40) only solutions with $\langle\varphi[f_0(980)]\rangle \simeq -67.5^\circ$ are kept.

The values of average mixing angles for $f_0(1300)$ are stable negative for both Solutions **I** and **II**, they differ slightly, so we may accept $\langle\varphi[f_0(1300)]\rangle = -10^\circ \pm 6^\circ$.

Also the mean mixing angle for the $f_0(1500)$ does not differ noticeably for Solutions **I** and **II**, so we may adopt $\langle\varphi[f_0(1500)]\rangle = 11^\circ \pm 8^\circ$.

For the $f_0(1750)$, Solutions **I** and **II** provide different mean values of mixing angle. In Solution **I**, the resonance $f_0(1750)$ is dominantly $s\bar{s}$ system; correspondingly, $\langle\varphi[f_0(1750)]\rangle = -72^\circ \pm 5^\circ$. In Solution **II**, the absolute value of mixing angle is much less, $\langle\varphi[f_0(1750)]\rangle = -18^\circ \pm 5^\circ$.

For the broad state, both Solutions give proximate values of mixing angle, namely, $\langle\varphi[f_0(1200-1600)]\rangle = 30^\circ \pm 3^\circ$. This magnitude favours the opinion that the broad state can be treated as the glueball descendant, because such a value of the mean mixing angle corresponds to $\varphi_{glueball} = \sin^{-1}\sqrt{\lambda/(2+\lambda)}$ at $\lambda \sim 0.50 - 0.85$.

Let us emphasize that the coupling magnitudes for the f_0-resonances found in [8] do not provide us any alternative variants for the glueball descendant. Indeed, the value which is the closest to the $\varphi_{singlet}$ is the limit value of the mean angle for $f_0(1500)$ in Solution **I**: $\langle\varphi[f_0(1500)]\rangle = 19^\circ$. Such a magnitude being used for the definition of $\varphi_{glueball}$ corresponds to $\lambda = 0.24$, but this suppression parameter is much lower than those observed in other processes: for the decaying processes we have $\lambda = 0.6 \pm 0.2$ [11, 22], while for the high-energy multiparticle production it is $\lambda \simeq 0.5$ [23]. In this way, the quark combinatorics points to the one candidate only, that is, the broad state $f_0(1200-1600)$; we come back to this important statement later on.

Generally, the formulae (38) allow us to find φ as a function of the coupling constant ratio G/g for the decays $glueball \to mesons$ and $q\bar{q}\text{-}state \to mesons$. The results of the fit for $f_0(980)$, $f_0(1300)$, $f_0(1500)$, $f_0(1750)$ and the broad state $f_0(1200-1600)$ are shown in Fig. 8.

First, consider the results for $f_0(980)$, $f_0(1300)$, $f_0(1500)$, $f_0(1750)$ shown in Fig. 8a for Solution **I** and in Fig. 8c for Solution **II**. The bunches of curves in the $(\varphi, G/g)$-plane demonstrate correlations between mixing angle values and the G/g ratios, for which the description of couplings given in Table 4 is satisfactory. A vague dissipation of curves, in particular noticeable for $f_0(1300)$ and $f_0(1500)$, is due to the uncertainty of λ in Eqs. (39) and (40).

The correlation curves in Fig. 8a,c allow one to see, on a qualitative level, to what extent the admixture of the gluonium component in $f_0(980)$, $f_0(1300)$, $f_0(1500)$, $f_0(1750)$ affects the quark-gluonium content, $q\bar{q} = n\bar{n}\cos\varphi + s\bar{s}\sin\varphi$ determined from

hadronic decays. The magnitudes g^2 and G^2 are proportional to the probability to find out, respectively, the quarkonium and gluonium components, $W_{q\bar{q}}$ and $W_{gluonium}$ in a considered resonance:

$$g^2 = g^2_{q\bar{q}} W_{q\bar{q}} \ , \qquad G^2 = G^2_{gluonium} W_{gluonium} \ . \tag{41}$$

The results of the K-matrix fit obtained in [8] tell us that the coupling constants $g^2_{q\bar{q}}$ and $G^2_{gluonium}$ are of the same order of magnitude (also see the discussion in [11, 64, 70]), therefore we accept as a qualitative estimate:

$$G^2/g^2 \simeq W_{gluonium}/W_{q\bar{q}} \ . \tag{42}$$

The figures 8a,c show the following permissible scale of values φ for the resonances $f_0(980)$, $f_0(1300)$, $f_0(1500)$, $f_0(1750)$, after mixing with the gluonium component.

Solution **I**:

$$\begin{aligned}
W_{gluonium}[f_0(980)] \lesssim 15\% \ : \qquad & -93^\circ \lesssim \varphi[f_0(980)] \lesssim -42^\circ, \\
W_{gluonium}[f_0(1300)] \lesssim 30\% \ : \qquad & -25^\circ \lesssim \varphi[f_0(1300)] \lesssim 25^\circ \ , \\
W_{gluonium}[f_0(1500)] \lesssim 30\% \ : \qquad & -2^\circ \lesssim \varphi[f_0(1500)] \lesssim 25^\circ \ , \\
W_{gluonium}[f_0(1750)] \lesssim 30\% \ : \qquad & -112^\circ \lesssim \varphi[f_0(1750)] \lesssim -32^\circ \ .
\end{aligned} \tag{43}$$

Solution **II**:

$$\begin{aligned}
W_{gluonium}[f_0(980)] \lesssim 15\% \ : \qquad & -90^\circ \lesssim \varphi[f_0(980)] \lesssim -43^\circ, \\
W_{gluonium}[f_0(1300)] \lesssim 30\% \ : \qquad & -42^\circ \lesssim \varphi[f_0(1300)] \lesssim 10^\circ \ , \\
W_{gluonium}[f_0(1500)] \lesssim 30\% \ : \qquad & -18^\circ \lesssim \varphi[f_0(1500)] \lesssim 23^\circ \ , \\
W_{gluonium}[f_0(1750)] \lesssim 30\% \ : \qquad & -46^\circ \lesssim \varphi[f_0(1750)] \lesssim 7^\circ \ .
\end{aligned} \tag{44}$$

The φ-dependence of G/g is linear for $f_0(980)$, $f_0(1300)$, $f_0(1500)$, $f_0(1750)$. Another type of the correlation takes place for the state which is the glueball descendant: the correlations curves for this case form in the $(\varphi, G/g)$-plane a typical cross. Just this cross appeared for the broad state $f_0(1200-1600)$ for both Solutions **I** and **II**, see Fig. 8b,d.

The appearance of glueball cross by correlation curves in the $(\varphi, G/g)$-plane is due to the formation mechanism of the quark-antiquark component in the gluonium state: in the transition $gg \to (q\bar{q})_{glueball}$ the state $(q\bar{q})_{glueball}$ is fixed by the value of λ. So the glueball descendant is the quarkonium-gluonium composition as follows:

$$gg \cos\gamma + (q\bar{q})_{glueball} \sin\gamma \ ,$$

where

$$(q\bar{q})_{glueball} \ = \ n\bar{n} \cos\varphi_{glueball} + s\bar{s} \sin\varphi_{glueball} \ ,$$

and $\varphi_{glueball} = \tan^{-1}\sqrt{\lambda/2} \simeq 26^\circ - 33^\circ$ for $\lambda \simeq 0.50 - 0.85$. The ratios of couplings for the transitions $gg \to \pi\pi, K\bar{K}, \eta\eta, \eta\eta'$ are the same as for the quarkonium $(q\bar{q})_{glueball} \to \pi\pi, K\bar{K}, \eta\eta, \eta\eta'$, so the study of hadronic decays only do not permit to fix the mixing angle γ. This property – similarity of hadronic decays for the states gg and $(q\bar{q})_{glueball}$ – implies a specific form of the correlation curve in the $(\varphi, g/G)$-plane: the gluonium cross. Vertical component of the gluonium cross means that the glueball descendant has a considerable admixture of the quark-antiquark component $(q\bar{q})_{glueball}$. Horizontal line of the cross corresponds to the dominant gg component. The value of λ which affects the cross-like correlation on the $(\varphi, g/G)$-plane is denoted from now on as $\lambda_{glueball}$. For Solution **I**, we have $\lambda_{glueball} = 0.55$, while for Solution **II** $\lambda_{glueball} = 0.85$.

At not a large shift of λ from its mean value $\lambda_{glueball}$, the coupling constants $f_0(1200 - 1600) \to \pi\pi, K\bar{K}, \eta\eta, \eta\eta'$ can be also described, with a reasonable accuracy, by Eq. (38); in this case correlation curves on the $(\varphi, g/G)$-plane take the form of hyperbola. Shifting the value of λ in $|\lambda - \lambda_{glueball}| \sim 0.2$ breaks the description of couplings of the broad state by formulae (38).

The cross-type correlation on the $(\varphi, g/G)$-plane in the description of coupling constants $f_0 \to \pi\pi, K\bar{K}, \eta\eta, \eta\eta'$ by formula (38) is a characteristic signature of the glueball or glueball descendant. And *vice versa*: the absence of the cross-correlation should point to the quark-antiquark nature of resonance. Therefore, the K-matrix analysis proves definitely that $f_0(1200 - 1600)$ is the gluonium descendant, while $f_0(980)$, $f_0(1300)$, $f_0(1500)$, $f_0(1750)$ cannot pretend to be the glueballs.

The analysis proves that $f_0(1300)$, $f_0(1500)$ are dominantly the $n\bar{n}$-systems. Still, in Solution **II** the $q\bar{q}$ component of the resonance $f_0(1300)$ may contain rather large $s\bar{s}$ component in the presence of the 30% gluonium admixture in this resonance. As to the $f_0(1500)$, the mixing angle $\langle\varphi[f_0(1500)]\rangle$ in the $q\bar{q}$ component may reach 25° at $G/g \simeq -0.6$ (Solution **I**) that is rather close to $\varphi_{glueball}$. However, in this case the description of coupling constants g_a^2 (Table 4) is attained as an effect of the strong destructive interference of the amplitudes $(q\bar{q}) \to two\,pseudoscalars$ and $gg \to two\,pseudoscalars$. This fact tells us that one cannot be tempted to interprete $f_0(1500)$ as the glueball descendant.

3.6 The light σ-meson: Is there a pole of the 00^{++}-wave amplitude?

Effective σ-meson is needed in nuclear physics as well as in effective theories of the low-energy strong interactions — and such an object exists in a sense that there exists rather strong interaction, which is realized by the scattering phase passing through the value $\delta_0^0 = 90^\circ$ at $M_{\pi\pi} \simeq 600 - 1000$ MeV. In the naive Breit–Wigner-resonance interpretation, this would correspond to an amplitude pole; but the low-energy $\pi\pi$ amplitude is a result of the interplay of singular contributions of different kinds (left-hand cuts as well as poles located highly, $f_0(1400-1600)$ included) , so a straightforward interpretation of the σ-meson as a pole may fail.

The question is whether the σ-meson exists as a pole of the 00^{++}-wave amplitude. (See also [76], where this problem was particularly underlined.) However, until now there is no definite answer to this question, though this point is crucial for meson systematics.

The consideration of the partial S-wave $\pi\pi$ amplitude, by accounting for left singularities associated with the t- and u-channel interactions, favours the idea of the pole at $\mathrm{Re}\, s \sim 4m_\pi^2$. The arguments are based on the analytical continuation of the K-matrix solution to the region $s \sim 0 - 4\mu_\pi^2$ [31].

In [31], the $\pi\pi$-amplitude of the 00^{++} partial wave was considered in the region $\sqrt{s} < 950\,\mathrm{MeV}$. The account for the left-hand singularities had been done within the method described in Section 3.10.2, namely, the K-matrix amplitude was fitted in the form

$$K(s) \;=\; \sum_{n=1}^{6} \frac{f_n}{s+s_n} + f + \frac{g^2}{M^2 - s}\;, \tag{45}$$

where f_n, f, s_n, g^2, M^2 are parameters. The left-hand cut was fitted to six pole terms; the pole at $s = M^2$ ($M \sim 900$ MeV) corresponds to $\delta_0^0 = 90^\circ$. The fitting was performed to the low-energy scattering phases, δ_0^0, at $\sqrt{s} < 450$ MeV, and the scattering length, a_0^0. In addition at $450 \le \sqrt{s} \le 950\,\mathrm{MeV}$ the value δ_0^0 was sewn with those found in the K-matrix analysis [9]: from this point of view the solution found in [31] may be treated as analytical continuation of the K-matrix amplitude to the region $s \sim 0 - 4m_\pi^2$. The analytical continuation of the K-matrix amplitude of such a type accompanied by simultaneous reconstruction of the left-hand cut contribution provided us with the characteristics of the amplitude as follows. The amplitude has a pole at

$$\sqrt{s} \;\simeq\; 430 - i325 \;\; \mathrm{MeV}\;, \tag{46}$$

the scattering length,

$$a_0^0 \;\simeq\; 0.22\, m_\pi^{-1}\;, \tag{47}$$

and the Adler zero at

$$\sqrt{s} \;\simeq\; 50 \;\mathrm{MeV}\;. \tag{48}$$

The errors in the definition of the pole in solution (46) are large, and unfortunately they are poorly controlled, for they are governed, in the main, by uncertainties when left-hand singularities are restored. As to experimental data, the position of pole is rather sensitive to the scattering length value, which in the fit [31] was taken in accordance to the paper [77]: $a_0^0 = 0.26 \pm 0.06\, m_\pi^{-1}$. As one can see, the solution [31] requires a small scattering length value: $a_0^0 \simeq 0.22\, m_\pi^{-1}$. New and much more precise measurements of the K_{e4}-decay [78] provided $a_0^0 = (0.228 \pm 0.015) m_\pi^{-1}$, that agrees completely with the value (47) obtained in [31]. Such a coincidence favours undoubtedly the pole position (46).

So, the N/D-analysis of the low-energy $\pi\pi$-amplitude sewn with the K-matrix one [9], provides us with the arguments for the existence of the light σ-meson. In a set of papers, by modelling the left-hand cut of the $\pi\pi$-amplitude (namely, by using

interaction forces or the t- and u-channel exchanges), the light σ-meson had been also obtained [28, 29, 30], but the mass values are widely scattered, e.g. in [79] the pole has been obtained at essentially larger masses, $\sqrt{s} \sim 600 - 900\,\mathrm{MeV}$.

The observation of the light σ-meson is aggravated by the existence of the Adler zero in the $\pi\pi$-amplitude near the $\pi\pi$-threshold. Therefore, as was emphasized above, for the reliable determination of the σ-meson it is necessary to study the $\pi\pi$-production in the annihilation and decay reactions (of the type of $p\bar{p} \to \pi\pi\pi$ and $D \to \pi\pi\pi$), where the Adler zero is absent. However, one should emphasize again, in the $p\bar{p}$-annihilation, where the statistics is rather high, the σ-meson is not seen, while in the reaction $D^+ \to \pi^+\pi^-\pi^+$ [25] the statistics is not sufficient for the reliable analysis of the low-energy $\pi\pi$-spectrum.

By discussing the search for the light σ-meson in the three-particle reactions, it is necessary to accentuate a requirement, had it been fulfilled, one can confidently confirm the discovery of this resonance. I mean the rescattering of pions in the final state. The matter is that the fitting to the near-threshold state, that is actually the σ-meson, should be carried out under the correct account for the unitarity at small masses of the $\pi\pi$-system, while the contribution of crossing channels (for example, resonance production) leads to the violation of unitarity. The account for rescatterings in the $\pi\pi$-channel reconstructs the two-particle unitarity. Besides, the rescatterings restore logarithmic singularities of the three-particle amplitude, that may affect significantly the region of small $\pi\pi$ masses, in particular, in the presence of heavy resonances. The effects of pion rescatterings were studied in [4], where the combined analysis of the Dalitz-plot has been done for the reactions $p\bar{p}(\text{at rest}) \to \pi^0\pi^0\pi^0, \pi^0\eta\eta$ — it appeared that they act rather strongly upon the region of small $\pi\pi$-masses, though they are not important for the analysis of resonances at 1300–1500 MeV, that was the main goal of the investigation performed in [4]. An opposite point of view, namely, the statement about the possibility to single out the signal from #-meson without taking account of rescatterings, was claimed in [80].

Concerning the problem of search for the light σ-meson in the three-particle reactions, an important point should be emphasized, which being fulfilled would allow us to speak with confidence about reliable determination of this state. This is rescattering of pions in the final state. The matter is that fitting to a near-threshold state, such as σ-meson, should be carried out with correct account for unitarity at small $\pi\pi$-masses; at the same time the contribution of crossing channels (for example, the production of resonances) violates the unitarity. The rescatterings in the $\pi\pi$-channel being accounted for restore the two-particle unitarity near the $\pi\pi$-threshold. Besides, rescatterings lead to logarithmic singularities of the three-particle amplitude, which in the presence of heavy resonances affect significantly the low-mass region. The effect of pion rescatterings were considered in [4] at simultaneous analysis of Dalitz-plots in the reactions $p\bar{p}(at\,rest) \to \pi^0\pi^0\pi^0, \pi^0\eta\eta$: it occurred that they affect strongly the low-mass region though being not important for the analysis of resonances at 1300–1500 MeV — the main scope of investigation in [4]. An opposite viewpoint, namely, one can reliably detect the σ-meson signal without accounting for $\pi\pi$-rescatterings, is presented in [80].

3.7 Systematics of scalar states on the (n, M^2)- and (J, M^2)-planes and the problem of basic multiplet $1^3P_0 q\bar{q}$

The figures 1,2 and 3 demonstrate linear behaviour of the $q\bar{q}$-meson trajectories in the (n, M^2)- and (J, M^2)-planes for a variaty of states. In this way, it would be instructive to juxtapose the nonet classification given by the K-matrix analysis [8, 9, 57] with the systematics of the $q\bar{q}$-states in the (n, M^2)- and (J, M^2)-planes.

3.7.1 The K-matrix classification of scalars and $q\bar{q}$-trajectories in the (n, M^2)-planes

Consider the variant which follows directly from the K-matrix calssification of bare states: let us accept that the light σ-meson does not reveal itself as the amplitude pole or, if it exists, it is an extra state for the $q\bar{q}$-systematics. For this case, the location of scalar states (f_0, a_0, K_0) on the (n, M^2) trajectories is shown in Fig. 9.

Figure 9a demonstrates the trajectories for the resonance states 00^{++}, 9^{++} and $\frac{1}{2}0^+$, while in Fig. 9b the trajectories for corresponding bare states are shown (recall that the doubling of the f_0-trajectories occurs due to the existence of two components, $s\bar{s}$ and $n\bar{n}$). It is seen that the trajectory slopes for bare and real states are nearly the same (in Fig. 9 the trajectory slope is $\mu^2 = 1.3\,\mathrm{GeV}^2$).

The state $f_0^{bare}(1580 \pm 50)$ certainly does not belong to any of f_0^{bare}-trajectories shown in Fig. 9b, the trajectories of the real f_0-states does not need the state $f_0(1200-1600)$ too. This is natural, provided the $f_0^{bare}(1580 \pm 50)$ is the glueball and $f_0(1200-1600)$ the glueball descendant.

Gluodynamical lattice calculations tell us that the lightest scalar glueball is located in the mass region 1550–1750 [62]. There are also other arguments in favour of just in this mass region one may encounter the gluonium: the estimate of the mass of soft (or effective) gluon points to the gluon mass $m_{gluon} \sim 700 - 1000\,\mathrm{MeV}$. Experimental estimations of the effective-gluon mass are based on the study of hadronic spectra in radiative decays $J/\psi \to \gamma + hadrons$ and $\Upsilon \to \gamma + hadrons$ [81, 82]; they give for the gluon mass the value 800–1000 MeV. The close values were obtained within model calculations of the quark-gluon interactions in the soft region giving the value 700–800 MeV for the effective-gluon mass [83, 84]. The lattice calculations of the effective gluon agree reasonably with these estimates: accordingly, $m_{gluon} \simeq 700\,\mathrm{MeV}$ [85]. It is natural to believe that the mass of the lightest scalar glueball is of the order of the double effective gluon mass, $M_{glueball} \sim 2m_{gluon}$.

One should pay attention to the fact that the resonances $f_0(980)$, $f_0(1500)$ and $f_0(1300)$, $f_0(1750)$ lay neatly on linear trajectories, with a slope which nearly coincides with slopes of isovector trajectories: ρ_J, a_J and π_J. This circumstance argues in favour of the admixture of the glueball components not leading to strong violation of the linear behaviour of trajectories, at least for the f_0-meson sector.

It would be pertinent to recall that in the K-matrix analyses [8, 9] three Solutions have been found denoted as **I**, **II-1** and **II-2**. Solutions **II-1** and **II-2** occurred to be close to each other in resonance characteristics; yet, in Solution **II-1** the $f_0^{bare}(1580)$ is the $q\bar{q}$-state, and the glueball mass is around 1250 MeV. We reject this Solution, for it contradicts both the linearity of f_0^{bare}-trajectories and gluodynamical calculation results.

Therefore, from the point of view of the classification of states on the (n, M^2)-trajectories, the scheme where the $f_0^{bare}(700 \pm 100)$ and its descendant, $f_0(980)$, are the lightest states in the $1^3P_0 q\bar{q}$ nonet looks self-consistent. This scheme agrees with the coupling constants for the transitions f_0^{bare}, a_0^{bare}, $K_0^{bare} \to \pi\pi, K\bar{K}, \eta\eta, \eta\eta'$ [8, 11, 57]. Moreover, model calculations of masses of the $q\bar{q}$-mesons also point to a possible location of the $1^3P_0 q\bar{q}$-nonet in the range 900–1300 MeV [86]. Still, by considering the nonet classification, the question arises about large $s\bar{s}$-component in the lightest $q\bar{q}$ state: 67% in $f_0^{bare}(700 \pm 100)$ and $(45-75)\%$ in $f_0(980)$. But it would be appropriate to recall that we have already faced similar situation in the pseudoscalar sector: the η-meson also contain a large $s\bar{s}$-component, about 40%. Both states, η-meson and $f_0^{bare}(700 \pm 100)$, are close to the flavour octet, and strong interaction in the flavour octet states may cause the large $s\bar{s}$ component in light mesons. In other words, the value of the $s\bar{s}$ component in lightest mesons depends on the structure of the short-range forces, and to determine the structure of forces is the goal of the analysis and the motivation to perform the systematics of meson states.

So the root of the matter is whether the σ-meson, if it exists, is the standard $q\bar{q}$-state, a partner to $f_0(980)$. Then the nonet of scalar mesons looks as follows: $f_0(300-500)$, $f_0(980)$, $a_0(980)$ and the low-lying κ meson, $\kappa(800-1000)$. The argument against this scheme is the systematics of the K-mesons in the (J, M^2) plane, that is discussed below.

3.7.2 Systematics of kaons in the (J, M^2) plane

The existence of the scalar κ-meson, with the mass 800-1000 MeV, is under discussion as long as the discussion of σ-meson, e.g. see [24] and references therein. The low-energy data on the πK-scattering are poor, and this is the main reason of uncertainty in the κ-meson problem. The K-matrix analysis of the πK-amplitude [57] does not supply us with unambigous answer, for there exist solutions without amplitude pole at 800-1000 MeV but there are also solutions with the pole at $\sim 1000\,\text{MeV}$ [57]. The K-matrix analysis of the high-statistics Crystal Barrel data on the reactions $p\bar{p} \to K\bar{K}\pi$ and $n\bar{p} \to K\bar{K}\pi$ does not require the κ-meson [8].

Let us turn to the systematics of kaon states on the (J, M^2) plane: such systematics of kaons brings additional argumets to the discussion of whether σ and κ mesons are the standard $q\bar{q}$ states, members of the $1^3P_0 q\bar{q}$ multiplets, or not.

In the kaonic sector, the experimental data are poor, and a complete picture of the kaon disposition on the trajectories with $J^P = 0^-, 2^-, 4^-, ...$ and $J^P = 1^+, 3^+, 5^+, ...$

cannot be unambigously reconstructed: in Fig. 10a,d a conventional picture is presented for the location of these trajectories. More definite is the situation in the sectors with $J^P = 0^+, 2^+, 4^+, ...$ and $J^P = 1^-, 3^-, 5^-...$, see Fig. 10b,c: here we know the states laying on the leading and first daughter trajectories — and just on these trajectories the κ meson should lay, provided it is the standard $q\bar{q}$-state.

In the sectors with $J^P = 0^-, 2^-, 4^-, \ldots$ and $J^P = 1^+, 3^+, 5^+, \ldots$ (Fig. 10a,d) the doubling of trajectories takes place because of the presence of two spin states: for example, two states with $J^P = 1^+$ are defined by the quantum numbers $(L = 1, S = 1)$ and $(L = 1, S = 0)$; likewise, two states $J^P = 2^-$ are formed by two sets of quantum numbers, $(L = 2, S = 1)$ and $(L = 2, S = 0)$. Figures 10a,d represent a conjectural disposition of trajectories and demonstrate how many unknown states (open circles) are present in the groups $J^P = 0^-, 2^-, 4^-$ and $J^P = 1^+, 3^+, 5^+$.

More reliably determined are the trajectories for the groups with $J^P = 0^+, 2^+, 4^+$ (Fig. 10b) and $J^P = 1^-, 3^-, 5^-$ (Fig. 10c), where, as was said above, the leading and first daughter trajectories are fixed firmly. The leading and first daughter trajectories in these groups are degenerate: the states $K_{2^+}(1430)$, $K_{4^+}(2045)$ and $K^*(890)$, $K_{3^-}(1780)$, $K_{5^-}(2380)$ lay on the common leading trajectory $\alpha_{leading}(J) \simeq 0.25 + 0.90\,M^2$ (the slope is in GeV units), and the states $K_{0^+}(1430)$, $K_{2^+}(1980)$ and $K^*(1680)$ lay on the common trajectory $\alpha_{daughter}(J) \simeq -2.0 + 0.90\,M^2$, where $J^P = 0^+, 1^-, 2^+, 3^-$.

Figure 10b demonstrates also the location of the κ meson: one can see that this state does not lay either on leading or daughter trajectories. In order to put the κ meson onto the $q\bar{q}$ trajectory, the existence of the 2^+ kaon with the mass ~ 1600 MeV is needed, but the analysis [63] does not point to the presence of tensor resonance in this mass region. The fact that there is no room for the κ meson on the (J, M^2) $q\bar{q}$-trajectories is the argument against the construction of the lowest scalar nonet by using the states $f_0(300-500)$, $f_0(980)$, $a_0(980)$ and $\kappa(800-1000)$, that is actually an indication that the κ meson does not exist.

3.8 Exotic scalar states, $f_0(1200-1600)$ and $f_0(300-500)$

Two scalar states, the broad resonance $f_0(1200-1600)$ and the light σ-meson $f_0(300-500)$, remain beyond the considered here $q\bar{q}$ classification that is based on the K-matrix analysis [8, 9]; they should be treated as exotic states.

The K-matrix analysis gives us an unambigous interpretation of the $f_0(1200-1600)$. This state is the descendant of a pure glueball which, by accumulating of widths of neighbouring scalar–isoscalar states, turned into the broad resonance. All comparatively narrow resonances from the region $\sim 1500\,$MeV (they are $f_0(1300)$, $f_0(1500)$ and $f_0(1750)$) fit well the $q\bar{q}$-trajectories in the (n, M^2) plane, so just the broad resonance $f_0(1200-1600)$ is an extra one from the point of view of the $q\bar{q}$-systematics.

The fact that the glueball turned into the broad state allows us to say that the

glueball is "melted". The idea that the bound state of gluons can disappear due to strong interaction in the soft region was brought out rather long ago [87]. However, the "melting" observed in the K-matrix analysis is a specific one: the transformation of the glueball into the broad state occurs as a result of the decay processes (transitions of resonances into real mesons) that takes place at large distances, of the order or greater than $R_{confinement}$. Besides, the amplitude pole associated with $f_0(1200-1600)$ did not go far away from the physical region: the resonance half-width, that defines the imaginary value of mass related to the pole, is of the order of 500–1000 MeV, so the pole occurs inside the hemicircle, where the analysis of experimental data allowed us to reconstruct the analytical amplitude (supposing the threshold singularities be correctly taken into account).

The transition of the lightest scalar glueball into the broad resonance $f_0(1200-1600)$ gives rise to a number of questions. The glueball tranformation into the broad resonance, is it a unique event (in a sense, an occasional event) or is this a common phenomenon for exotic states? The resonance $f_0(1200-1600)$, after having accumulated the widths of neighbouring $q\bar{q}$-states plays, with respect to them, the role of a locking state, does this lead to the increase of the proper size of $f_0(1200-1600)$? These questions were put in [10, 71]; still, to have a veracious response one needs much more accurate data. Qualitative evaluation of the radius of $f_0(1200-1600)$ had been carried out in [10, 71, 72], on the basis of the GAMS data for the $M_{\pi\pi}$-distributions at different momenta transferred to the nucleon in the reaction $\pi^- p \to n\pi^0\pi^0$ at $p_{lab} = 38\,\mathrm{GeV/c}$ [12]. According to this estimate, the broad state is much more loosely-bound system than its neighbours-resonances. Recent measurements performed by the E852 Collaboration [18] support the fact that comparatively narrow resonances $f_0(980)$ and $f_01300)$ are more compact than the broad state $f_0(1200-1600)$; the discussion of these data can be found in [8, 52].

The situation with the light σ-meson, $f_0(300-500)$, is less definite as concern its experimental status and the understanding of its nature. The nature of the σ-meson, if it exists as an amplitude pole, is rather enigmatic. The light σ-meson is hardly the glueball-like formation. Also it is difficult to imagine the light σ-meson to be the standard $q\bar{q}$-system: the arguments against such an interpretation were formulated in Section 3.8.

It was suggested in [88] that the existence of the light σ-meson may be due to a singular behaviour of the forces between quark and antiquark at large distances (in quark models they are conventionally called "confinement forces"). The scalar confinement potential, which defines the spectrum of the $q\bar{q}$-states in the region 1000–2000 MeV, behaves at large hadronic distances as $V^{(c)}_{confinement}(r) \sim \alpha r$, where $\alpha \simeq 0.19\,\mathrm{GeV}^2$. In the momentum representation, such a growth of the potential is associated with the singular behaviour at small q:

$$V^{(c)}_{confinement}(q) \;\sim\; \frac{1}{q^4}\,. \tag{49}$$

In the colour space, the main contribution comes from the component $c = 8$, i.e.

the confinement forces should be the octet ones. The question that is crucial for the structure of σ-meson is as follows: is there a component with the colour singlet, $V^{(1)}_{confinement}(q)$, in the singular potential (49)? If the singular component with $c = 1$ exists, then it must reveal itself in hadronic channels as well, that is, in the $\pi\pi$-channel. In hadronic channels, this singularity should not be exactly the same as in the colour octet ones, because the hadronic unitarization of the amplitude (which is absent in the channel with $c = 8$) should modify somehow the low-energy amplitude. One may believe that, as a result of the unitarization in the channel $c = 1$, i.e. due to the account for hadronic rescatterings, the singularity of $V^{(1)}_{confinement}(q)$ may appear in the $\pi\pi$-amplitude on the second sheet and one may believe that this singularity is what we call "the light σ-meson".

Therefore, the main question consists in the following: the $V^{(1)}_{confinement}(q^2)$, does it have the same singular behaviour as $V^{(8)}_{confinement}(q^2)$? The observed linearity of the (n, M^2)-trajectories, up to the large-mass region, $M \sim 2000 - 2500$ MeV, see Figs. 1 and 2, favours the idea of the universality in the behaviour of potentials $V^{(1)}_{confinement}$ and $V^{(8)}_{confinement}$ at large r, or small q. To see that (for example, in the process $\gamma^* \to q\bar{q}$, Fig. 11a) let us discuss the colour neutralization mechanism of outgoing quarks as a break of the gluonic string by newly born $q\bar{q}$-pairs. At large distances, (2.0–2.5 fm), that corresponds to the formation of states with masses 2000–2500 MeV, two–three new $q\bar{q}$-pairs should be formed. This follows from the value $\langle n_{ch}(W)\rangle$ in the e^+e^--annihilation: at $W \simeq 2$ GeV we have $\langle n_{ch}\rangle \simeq 3$. It is natural to suggest that a convolution of the quark–gluon combs governs the interaction forces of quarks at large distances, see Fig. 11bc. This means that the potential $V^{(c)}_{confinement}$ working at such large distances contains two or three t-channel $q\bar{q}$-pairs. The mechanism of the formation of new $q\bar{q}$-pairs to neutralize colour charges does not have a selected colour component, see e.g. [89]. In this case all colour components $3 \otimes \bar{3} = 1 + 8$ behave similarly, that is, at small q^2 the singlet and octet components of the potential are uniformly singular, $V^{(1)}_{confinement}(q^2) \sim V^{(8)}_{confinement}(q^2) \sim 1/q^4$. This is seen in Fig. 11a: the quark–gluon ladder ensures the t-channel flow of colour charge $C = 3$, so quark–antiquark interaction block being the convolution of ladder diagrams $3 \otimes \bar{3} = 1 + 8$ contains two equivalent, singlet and octet, components. This points to a similarity of $V^{(1)}_{confinement}$ and $V^{(8)}_{confinement}$.

So, from the point of view of mechanisms of colour neutralization related to the ideas of the t-channel production of new quark–antiquark pairs, the existence of the light σ-meson is well-grounded. Therefore, it is of utmost importance to discover whether there exist singularities at low energies in the 00^{++}-amplitude, which we call the light σ-meson, and what is the type of these singularities, if any.

4 Conclusion

Recent analysis of meson spectra in the $p\bar{p}$-annihilation in flight [6] resulted in the opportunity to systematize $q\bar{q}$-mesons, practically leaving too small a room for speculations about the existence of exotic states. First of all, this is related to the 00^{++} sector, where all comparatively narrow resonances $f_0(980)$, $f_0(1300)$, $f_0(1500)$, $f_0(1750)$ lay on linear $q\bar{q}$-trajectories on the (n, M^2)- and (J, M^2) planes, that does not provide us with a ground for hypotheses on their exotic origin.

In quark models of 60–70's the idea of dominant **LS**-splitting was pushed forward [90, 91] — within such a structure of forces the P-wave $q\bar{q}$-multiplet with $J = 0$ is lighter than multiplets with $J = 1, 2$. Recently the models became popular, where $f_0(980)$ and $a_0(980)$ are considered as exotic states (see [92, 93, 94] and references therein): in this case the $1^3P_0 q\bar{q}$-nonet should be placed in the region 1300–1700 MeV. It is seen that the K-matrix analysis [8,11,12,13] renders us back to a former picture: the $1^3P_0 q\bar{q}$ multiplet is the lightest one among the P-wave $q\bar{q}$-states.

Beyond the 00^{++} sector, the candidate for the exotics is the $\pi_2(1880)$ [39] — for sure this state does not belong definitely to the $q\bar{q}$-trajectory, and it could be a hybrid state. Of course, the existence of this resonance should be confirmed by its observation in other reactions. Besides, if $\pi_2(1880)$ was the $q\bar{q}g$-state, there should exist the other nonet members near 1900 MeV in addition to those that lay on standard (n, M^2) trajectories. However, no 2^{-+} mesons have been observed yet, which could be extra ones with respect to the $q\bar{q}$ classification.

In the literature, there are indications to a plausible existence of the non-quark-antiquark mesons with $J^{PC} = 1^{-+}$ (see [19] and references therein), though experimental evidence for these states is rather poor.

In the 00^{++} meson sector, two states are beyond the $q\bar{q}$ systematics, namely, the light σ-meson and the broad state $f_0(1200 - 1600)$.

Concerning the problem of the light σ-meson, though important and having a long discussion history, there is no direct evidence of its existence — on the level of fixing a pole in the 00^{++} amplitude on the basis of the experimental data with large statistics. Such a situation existed a few years ago, see the discussion in [76], yet there is no noticeable experimental progress till now.

Nevertheless there are reasons which make us to concern about the problem of the light σ-meson: this is singular behaviour of the quark–antiquark interaction block at small momentum transfers, $1/q^4$, in the coordinate space this corresponds to the linear growth of the potential, $\sim \alpha r$, at large r (in quark models such a potential is conventionally called "confinement potential"). Linear behaviour of meson trajectories in the (n, M^2)-plane at large masses (Figs. 1,2) tells us that such a behaviour occurs actually at rather large r, up to $r \sim 2.0 - 2.5$ fm. Assuming that both colour components of the "confinement potential", octet and singlet ones, behave at large r similarly, $V^{(1)}_{octet}(r) \sim V^{(8)}_{singlet}(r)$, we gain singular behaviour at small masses in the

white (hadronic) channel. Hadron unitarization of the amplitude (the account for the $\pi\pi$-rescatterings), which is necessary in the white channel but is absent in colour one, is capable to "hide" the white-channel singularity under the $\pi\pi$ branching cut thus re-creating the picture of the light σ-meson. The mechanism of colour neutralization, where the t-channel formation of new $q\bar{q}$ pairs is of principal importance, favours the hypothesis about similar growth of potentials $V^{(1)}_{confinement}(r) \sim V^{(8)}_{confinement}(r)$.

As concern the broad state $f_0(1200-1600)$, we know neither its mass nor the width reliably. Still, we do know that this broad state is strongly produced in a number of reactions. Also we know that, in terms of the $q\bar{q}$ and gluonium components, this state is for sure the mixture of the gluonium with the quark-antiquark state which is close, by its content, to the flavour singlet $(q\bar{q})_{glueball} = (n\bar{n}\sqrt{2} + s\bar{s}\sqrt{\lambda})/\sqrt{2+\lambda}$ with $\lambda \simeq 0.5 - 0.8$: this fact is proved rather confidently by the relations between the couplings $f_0(1200-1600) \to \pi\pi, K\bar{K}, \eta\eta, \eta\eta'$, which are reliably found from the data.

Another reliably determined feature of the broad state $f_0(1200-1600)$ is that it is a more loosely-bound system than the surrounding f_0-resonances; this fact points to a possibility to create it as a result of the accumulation of widths of neighbouring resonances. If so, and the K-matrix analyses of the 00^{++} waves [8, 9] performed on an extended data basis favours this scenario, then this circumstance explains us where the lightest scalar glueball vanishes, though it promised to be around ~ 1500 MeV but it is definitely missing among the observed narrow f_0-mesons. In this way, let us emphasize that the possibility for a new comparatively narrow 00^{++} resonance near 1000-1800 MeV is strictly excluded by the available experimental data.

A scenario for $f_0(1200-1600)$ being the glueball descendant, which lost a part of its gluonium component due to the mixing with neighbouring resonances, was suggested in [68, 69], on the basis of data which were much poorer than the present ones. The nowaday data which are richer not only in statistics but also in a number of investigated reactions, fit to this picture rather well, without noticeable contradictions to it. One more check of the picture with $f_0(1200-1600)$ as a glueball descendant is expected in the nearest future for the high-statistics radiative decays $J/\Psi \to \gamma + hadrons$: in hadronic spectra, the production of comparatively narrow resonances $f_0(1300)$ and $f_0(1500)$ in the 00^{++} wave should be accompanied by a strong "background" due to the production of the broad state $f_0(1200-1600)$.

At the time being the mixing of f_0-mesons at 1300–1700 MeV is intensively discussed, see recent papers [95, 96] as an example. However, it should be specially stressed that the mixing considered in the K-matrix technique is in principle different from mixing discussed in [95, 96]. In the K-matrix approach, the mixing occurs due to transitions of bare states to real mesons — in other words, due to imaginary parts of hadron loop diagrams. As a result of such a mixing the amplitude poles "move" in the complex mass plane, a loss or accumulation of widths take place, that is, mixed states "push" each other in the complex plane by sinking deeply into complex plane or springing out to real axis; as a result, real mesons-resonances are created. In this way the shift of real part of resonance mass may be considerable — of the order of

resonance width. The mixing discussed in the papers [95, 96] happens without decay processes, that is, without imaginary parts of hadronic loop diagrams, so corresponding amplitude poles are on real axis: by mixing the levels repulse each other, with the increase or decrease of the mass but not width; after such a mixing the bare states should be created but not real resonances, as was suggested in papers [95, 96]. Once again: in the K-matrix technique the formation of the observed resonances takes place by the onset of the decay processes only.

In accordance with gluodynamical lattice calculations, the second scalar glueball should exist at 2100–2200 MeV [97]. In [98], it was suggested that $f_0(2105)$ is either this second glueball or strongly mixed with it. However there is not enough data to judge about the glueball being in this mass region: the discovered resonances lay on the $q\bar{q}$ trajectories quite comfortably. It is rather probable that the second scalar glueball turned into the broad state too by mixing with the neighbouring $q\bar{q}$ mesons — in this case to fix it experimentally the measurement of a large variety of spectra is needed as well as the evaluation of ratios for the $\pi\pi$, $K\bar{K}$, $\eta\eta$, $\eta\eta'$, $\eta'\eta'$ yields in the region 2100–2200 MeV.

Acknowledgement

I am indebted to A.V. Anisovich, Ya.I. Azimov, D.V. Bugg, L.G. Dakhno, Yu. S. Kalashnikova, D.I. Melikhov, V.A. Nikonov and A.V. Sarantsev for helpful discussions of problems involved. This work is supported by the RFBR Grant N 0102-17861.

References

[1] A.V. Anisovich, V.V. Anisovich, V.A. Nikonov, and A.V. Sarantsev, *"Meson spectrum from analysis of the Crystal Barrel data"*, in: *"PNPI XXX, Scientific Highlights, Theoretical Physics Division"*, p. 58, Gatchina (2001).

[2] V.V. Anisovich, D.V. Bugg, A.V. Sarantsev, B.S. Zou, Yad. Fiz. **57** 1666 (1994) [Phys. Atom. Nucl. **57**, 1595 (1994)].

[3] V.V. Anisovich, D.S. Armstrong, I. Augustin, *et al.*, Phys. Lett. B **323**, 233 (1994).

[4] V.V. Anisovich, D.V. Bugg, A.V. Sarantsev, B.S. Zou, Phys. Rev. D **50**, 1972 (1994).

[5] C. Amsler, V.V. Anisovich, D.S. Armstrong *et al.*, Phys. Lett. B **333**, 277 (1994); D.V. Bugg, V.V. Anisovich, A.V. Sarantsev, B.S. Zou, Phys. Rev. D **50**, 4412 (1994).

[6] A.V. Anisovich, C.A. Baker, C.J. Batty *et al.*, Phys. Lett. B**449**, 114 (1999); B**452**, 173 (1999); B **452**, 180 (1999); B **452**, 187 (1999); B **472**, 168 (2000); B

476, 15 (2000); B **477**, 19 (2000); B **491**, 40 (2000); B **491**, 47 (2000); B **496**, 145 (2000); B **507**, 23 (2001); B **508**, 6 (2001); B **513**, 281 (2001); B **517**, 261 (2001); B **517**, 273 (2001);
Nucl. Phys. A **651**, 253 (1999); A **662**, 319 (2000); A **662**, 344 (2000).

[7] A.V. Anisovich, V.V. Anisovich, and A.V. Sarantsev, Phys. Rev. D **62**:051502 (2000).

[8] V.V. Anisovich, A.V. Sarantsev, Eur. Phys. J. A**16**, 229 (2003).

[9] V.V. Anisovich, A.A. Kondashov, Yu.D. Prokoshkin, S.A. Sadovsky, A.V. Sarantsev, Yad. Fiz. **60** 1489 (2000) [Physics of Atomic Nuclei **60** 1410 (2000)].

[10] V.V. Anisovich, D.V. Bugg and A.V. Sarantsev, Yad. Fiz. **62** 1322 (1999); [Phys. Atom. Nuclei, **62** 1247 (1999)].

[11] V.V. Anisovich, UFN **168** 481 (1998) [Physics-Uspekhi, **41** 419 (1998)].

[12] D. Alde *et al.*, Zeit.Phys. C **66** 375 (1995);
Yu.D. Prokoshkin *et al.*, Physics – Doklady **342** 473 (1995);
A.A. Kondashov *et al.*, Preprint IHEP 95-137, Protvino, 1995.

[13] F. Binon *et al.*, Nuovo Cim. A **78** 313 (1983); **80** 363 (1984).

[14] S.J. Lindenbaum and R.S. Longacre, Phys. Lett. B **274** 492 (1992);
A. Etkin *et al.*, Phys. Rev. D **25** 1786 (1982).

[15] G. Grayer *et al.*, Nucl. Phys. B **75** 189 (1974);
W. Ochs, PhD Thesis, Münich University (1974).

[16] C. Amsler et al., Phys. Lett. B **342**, 433 (1995); B **355**, 425 (1995).

[17] A. Abele et al., Phys. Rev. D **57**, 3860 (1998); Phys. Lett. B **391**, 191 (1997); B **411**, 354 (1997); B **450**, 275 (1999); B **468**, 178 (1999); B **469**, 269 (1999);
K. Wittmack, PhD Thesis, Bonn University, (2001);
E. Klempt and A.V. Sarantsev, private comminication.

[18] J. Gunter et al. (E852 Collaboration), Phys. Rev. D **64**:07003 (2001).

[19] D.E. Groom *et al.* (Particle Data Group), Eur. Phys. J. C **15**, 1 (2000).

[20] V.V. Anisovich and A.V. Sarantsev, Phys. Lett. B **382** 429 (1996).

[21] A.V. Anisovich, *Quark/gluon content of η(1295) and η(1440)*, hep-ph/0104005 (2001).

[22] K. Peters and E. Klempt, Phys. Lett. B **352**, 467 (1995).

[23] V.V. Anisovich, M.G. Huber, M.N. Kobrinsky, and B.Ch. Metsch, Phys. Rev. D **42**, 3045 (1990).

[24] E. van Beveren and G. Rupp, *Scalar mesons within a model for all nonexotic mesons*, in Proceedings of the Workshop on Recent Developments in Particle and Nuclear Physics, April 30, 2001, Coimbra (Portugal) ISBN 972-95630-3-9, pages 1-16, hep-ph/0201006 (2002);
S. Spanier, N.A. Törnqvist, Eur. Phys. J. C **15** 437 (2000).

[25] E.M. Aitala et al., Phys. Rev. Lett. **86** 770 (2001); **86** 779 (2001).

[26] N. Wu et al. (BES collaboration) *BES measurements and J/Ψ decays*, Talk given at 36th Rencontres de Moriond on QCD and Hadronic Interactions, Les Arcs, France, 17-24 Mar 2001, hep-ex/0104050 (2001).

[27] D.M. Asner et al., (CLEO collaboration), Phys. Rev. D **61**:0120002 (2001).

[28] J.L. Basdevant, C.D. Frogatt, J.L. Petersen, Phys. Lett. B **41** 178 (1972);
D. Iagolnitzer, J. Justin, J.B. Zuber, Nucl. Phys. B **60** 233 (1973).

[29] E. van Beveren et al., Phys. Rev. C **30**, 615 (1986).

[30] B.S. Zou, D.V. Bugg, Phys. Rev. D **48**, R3942 (1994); D **50** 591 (1994);
G. Janssen, B.C. Pearce, K. Holinde, J. Speth, Phys. Rev. D **52** 2690 (1995);
N.A. Törnquist and M. Roos, Phys. Rev. Lett. **76** 1575 (1996);
A. Dobado and J.R. Peláez, Phys. Rev. D **56** 3057 (1997);
M.P. Locher, V.E. Markushin and H.Q. Zheng, Eur. Phys. J. C **4** 317 (1998);
J.A. Oller, E. Oset and J.R. Peláez, Phys. Rev. D **59**:074001 (1999);
Z. Xiao and H.Q. Zheng, Nucl. Phys. A **695** 273 (2001).

[31] V.V. Anisovich and V.A. Nikonov, Eur. Phys. J. **A8** 401 (2000).

[32] E. Aker *et al.*, Phys.Lett. B **260** 249 (1991).

[33] V.V. Anisovich, A.A. Anselm, V.N. Gribov, Nucl. Phys. **38** 132 (1962);
V.V. Anisovich, A.A. Anselm, UFN **88** 287 (1965).

[34] I.J.R. Aitchison, Phys. Rev. **133** 1257 (1964);
B.N. Valuev, ZETP **47** 649 (1964). [Sov. Phys. JETP **20** 433 (1964);
V.V. Anisovich, L.G. Dakhno, Phys. Lett. **10** 221 (1964); Nucl. Phys. **76** 657 (1966);
M.N. Kobrinsky and A.K. Likhoded, Yad. Fiz. **17** 1973 (1973) [Sov. J. Nucl. Phys. **17** 683 (1973)].

[35] A.V. Anisovich, V.V. Anisovich, Yad. Fiz. **53** 1485 (1991). [Sov. J. Nucl. Phys. **53** 915 (1991)]; Phys. Lett. B **345** 321 (1995).

[36] V.V. Anisovich, Yu.D. Prokoshkin, and A.V. Sarantsev, Phys. Lett. B **389** 388 (1996).

[37] A.V. Anisovich, D.V. Bugg, N. Djaoshvili et al., Nucl. Phys. A **690** 567 (2001).

[38] A.V. Sarantsev, private communication.

[39] A.V. Anisovich, C.A. Baker, C.J. Batty *et al.*, Phys. Lett. B **500** 222 (2001).

[40] P. Minkowski, W. Ochs, Eur. Phys. J. C **9** 283 (1999).

[41] L. Montanet, Nucl. Phys. Proc. Suppl. **86** 381 (2000).

[42] C.M. Shakin and H. Wang, Phys. Rev. D **63**:014019 (2000).

[43] E. Klempt, *Meson spectroscopy: glueballs, hybrids and $q\bar{q}$ mesons*, in "Zuoz 2000, Phenomenology of gauge interactions" 61-126, hep-ex/0101031 (2001).

[44] R. Kamenski, L. Lesniak, and K. Rubicki, Eur.Phys.J.direct **C4** 4 (2002).

[45] F.E. Close and N.A. Törnqvist, J.Phys. **G28** R249 (2002).

[46] M.V. Polyakov and V.V. Vereshagin, Eur. Phys. J. A **12** 349 (2001);
A.V. Sarantsev, private communication.

[47] K.M. Watson, Phys. Rev. **88**, 1163 (1952);
A.B. Migdal, Zh. Exp. Theor. Fiz. **28**, 10 (1955).

[48] A.V. Anisovich, V.V. Anisovich, V.N. Markov, M.A. Matveev, and A.V. Sarantsev, J. Phys. G: Nucl. Part. Phys. **28**, 15 (2002).

[49] C. Zemach, Phys. Rev. **140**, B97 (1965); **140**, B109 (1965).

[50] S.-U. Chung, Phys. Rev. D **57**, 431 (1998).

[51] A.V. Anisovich, Yad. Fiz. **66**, 175 (2003) [Phys. Atom. Nucl.**66** 172 (2003)].

[52] V.V. Anisovich and A.V. Sarantsev, Yad. Fiz. **66** 960 (2003) [Phys. Atom. Nucl. **66** 9280 (2003)].

[53] V.V. Anisovich, A.A. Kondashov, Yu.D. Prokoshkin, S.A. Sadovsky, and A.V. Sarantsev, Phys. Lett. B **355** 363 (1995).

[54] N.N. Achasov and G.N. Shestakov, Yad. Fiz. **62**, 548 (1999) [Phys. Atom. Nucl.**62** 505 (1999)]..

[55] J. Orear, Phys. Lett. **13** 190 (1964).

[56] N.N. Achasov and G.N. Shestakov, Phys.Lett. **B528** 73 (2002).

[57] A.V. Anisovich and A.V. Sarantsev, Phys.Lett. B **413** 137 (1997).

[58] G. t'Hooft, Nucl. Phys. B **72**, 461 (1974);
G. Veneziano, Nucl. Phys. B **117**, 519 (1976).

[59] V.V. Anisovich and V.M. Shekhter, Nucl. Phys. **B55**, 455 (1973);
J.D. Bjorken and G.E. Farrar, Phys. Rev. D **9**, 1449 (1974).

[60] M.A. Voloshin, Yu.P. Nikitin, and P.I. Porfirov, Yad. Fiz. **35** 1006 (1982) [Sov. J. Nucl. Phys. **35**, 586 (1982)].

[61] S.S. Gershtein, A.K. Likhoded, Yu.D. Prokoshkin, Zeit. Phys. **C24**, 305 (1984);
C. Amsler and F.E. Close, Phys. Rev. D **53**, 295 (1996); Phys. Lett. B **353**, 385 (1995);
V.V. Anisovich, Phys. Lett. B **364**, 195 (1995).

[62] G.S. Bali et al., Phys. Lett. B **309** 378 (1993);
J. Sexton, A. Vaccarino, and D. Weingarten, Phys. Rev. Lett. **75** 4563 (1995);
C.J. Morningstar, M. Peardon, Phys. Rev. D **56** 4043 (1997).

[63] D. Aston *et al.* Nucl. Phys. B **296** 493 (1988).

[64] A.V. Anisovich, V.V. Anisovich, and A.V. Sarantsev, Zeit. Phys. A **359**, 173 (1997).

[65] I.S. Shapiro, Nucl. Phys. A **122** 645 (1968).

[66] I.Yu. Kobzarev, N.N. Nikolaev, and L.B. Okun, Yad. Fiz. **10** 864 (1970) [Sov. J. Nucl. Phys. **10** 499 (1970)].

[67] L. Stodolsky, Phys. Rev. D **1** 2683 (1970).

[68] A.V. Anisovich, V.V. Anisovich, Yu.D. Prokoshkin, and A.V. Sarantsev, Zeit. Phys. A **357** 123 (1997).

[69] A.V. Anisovich, V.V. Anisovich, A.V. Sarantsev, Phys. Lett. B **395** 123 (1997).

[70] V.V. Anisovich, UFN **165**, 1225 (1995) [Physics-Uspekhi **38**, 1179 (1995)].

[71] V.V. Anisovich, D.V. Bugg, and A.V. Sarantsev, Phys. Rev. D **58**:111503 (1998).

[72] V.V. Anisovich, D.V. Bugg, and A.V. Sarantsev, Phys. Lett. B **437** 209 (1998).

[73] V.V. Anisovich, V.A. Nikonov, and A.V. Sarantsev, Yad. Fiz. **66**, 772 (2003); [Phys. Atom. Nucl. **66**, 741 (2003)].

[74] Anisovich V V, Bugg D V, Melikhov D I, Nikonov V A. *Phys. Lett. B* **404** 166 (1997)

[75] Anisovich V V, Montanet L, Nikonov V A. *Phys. Lett. B* **480** 19 (2000)

[76] M.R. Pennington, *"Riddle of the scalars: where is the σ?"*, in: Frascati Physics Series **XV**, 95 (1999).

[77] L. Rosselet et al., Phys. Rev. D **15**, 576 (1977);
O. Dumbraits, et al., Nucl. Phys. B **216**, 277 (1983).

[78] S. Pislak et al., Phys.Rev.Lett. **87** 221801 (2001).

[79] S.D. Protopopescu *et al.*, Phys. Rev. D **7** 1279 (1973);
P. Estabrooks, Phys. Rev. D **19** 2678 (1979);
K.L. Au, D. Morgan, and M.R. Pennington, Phys. Rev. D **35** 1633 (1987);
S. Ishida *et al.*, Prog. Theor. Phys. **98** 1005 (1997).

[80] M. Ishida, Prog.Theor.Phys.Suppl. **149** 190 (2003).

[81] G. Parisi, R. Petronzio, Phys. Lett. B **94** 51 (1980).

[82] M. Consoli, J.H. Field, Phys. Rev. D **49** 1293 (1994).

[83] J.M. Cornwell, J. Papavassiliou, Phys. Rev. D **40** 3474 (1989).

[84] V.V. Anisovich, S.M. Gerasyuta, A.V. Sarantsev, Int. J. Mod. Phys. A **6** 2625 (1991).

[85] D.B. Leinweber *et al.*, Phys. Rev. D **58** 031501 (1998).

[86] R. Ricken, M. Koll, D. Merten, B.C. Metsch, and H.R. Petry, Eur. Phys. J. A **9**, 221 (2000).

[87] C.A. Heusch, *"Gluonium — an unfulfilled promise of QCD?"* in: QCD-20 Years later, eds. P.M. Zerwas, H.A. Kastrup, Singapore, World Scientific, 1993.

[88] V.V. Anisovich and V.A. Nikonov, *The low-mass σ-meson: Is it an eyewitness of confinement?*, hep-ph/0008163 (2000).

[89] V.V. Anisovich, M.N. Kobrinsky, J. Nyiri, and Yu.M. Shabelski, *"Quark Model and High Energy Collisions"*, World Scientific, Singapore, 1985.

[90] Ya.B. Zeldovich, A.D. Sakhorov, Yad. Fiz. **4**, 395 (1966) [Sov. J. Nucl. Phys. **4**, 283 (1967)].

[91] A. deRujula, H. Georgi, and S.L. Glashow, Phys. Rev. D **12**, 147 (1975).

[92] R.L. Jaffe, Phys. Rev. D **15**, 267 (1977); **15**, 281 (1977).

[93] J. Weinshtein and N. Izgur, Phys. Rev. D **41**, 2236 (1990).

[94] H.Y. Cheng, Phys.Rev.D **67** 034024 (2003).

[95] F.E. Close and A. Kirk, Eur. Phys. J. C **21**, 531 (2001).

[96] W. Lee and D. Weingarten, Phys. Rev. D **61** 014015 (2000).

[97] C.J. Morningstar and M. Peardon, Phys. Rev. D**60**:034509 (1999).

[98] D.V. Bugg, M. Peardon, and B.S. Zou, Phys. Lett. B **486**, 49 (2000).

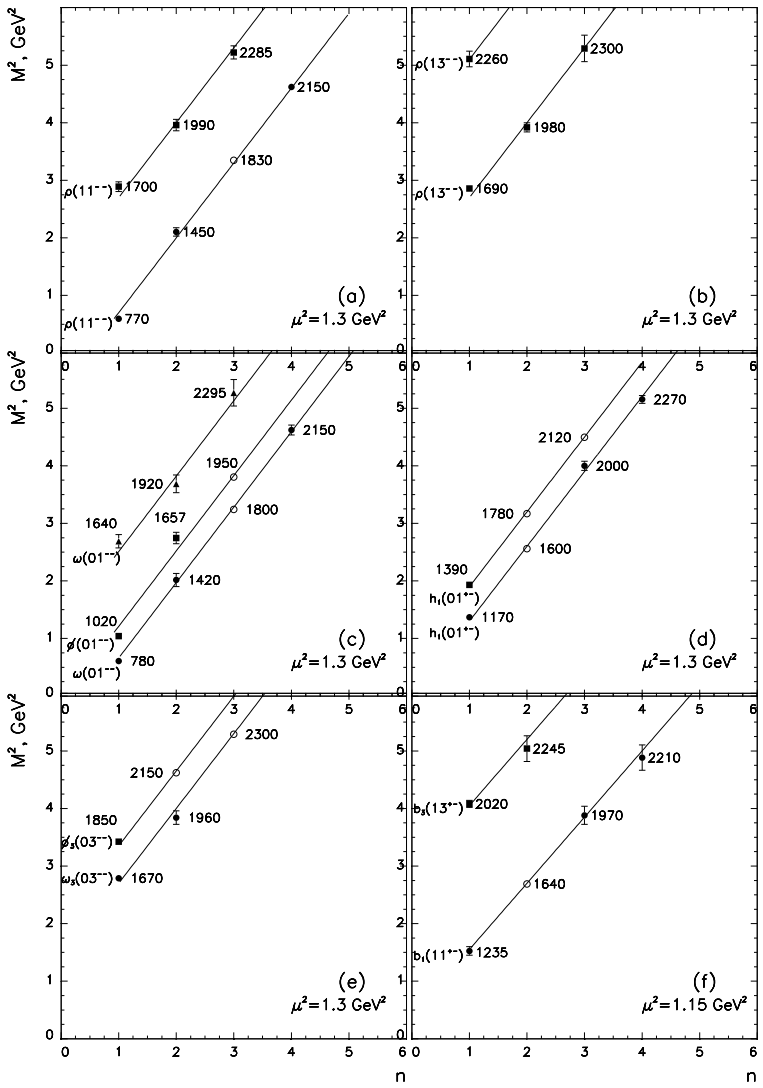

Figure 1: Trajectories on the (n, M^2) planes for the states with $(C = -)$. Open circles stand for the predicted states.

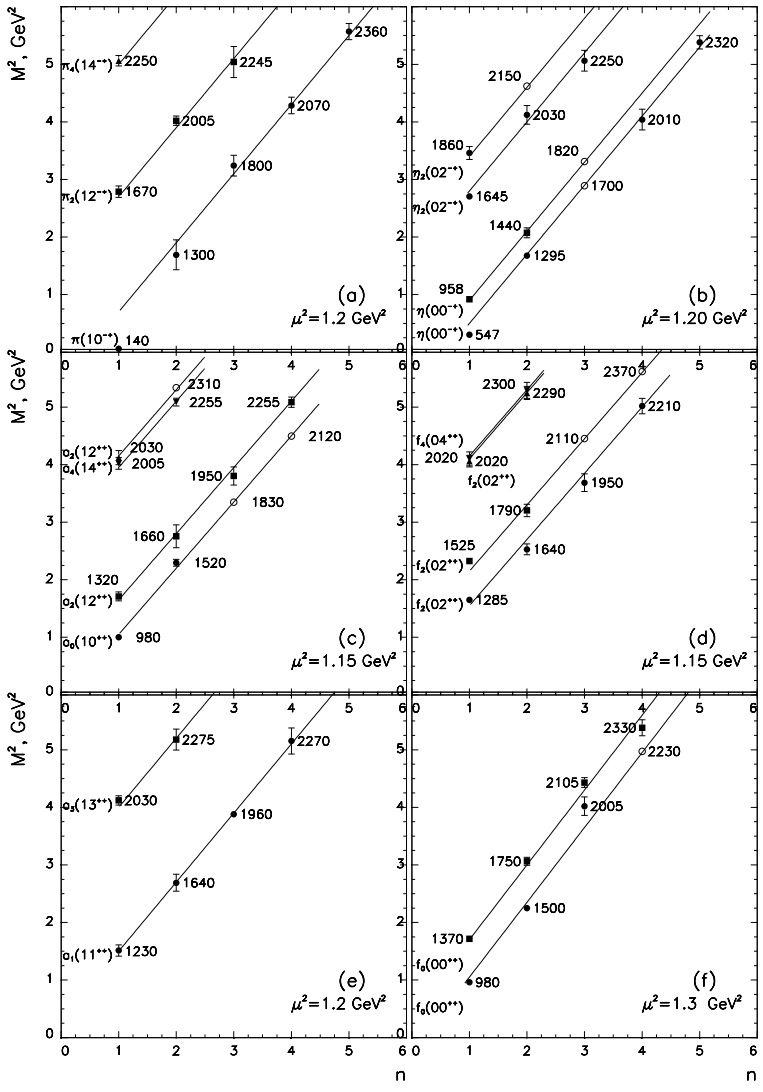

Figure 2: Trajectories on the (n, M^2) planes for the states with $(C = +)$.

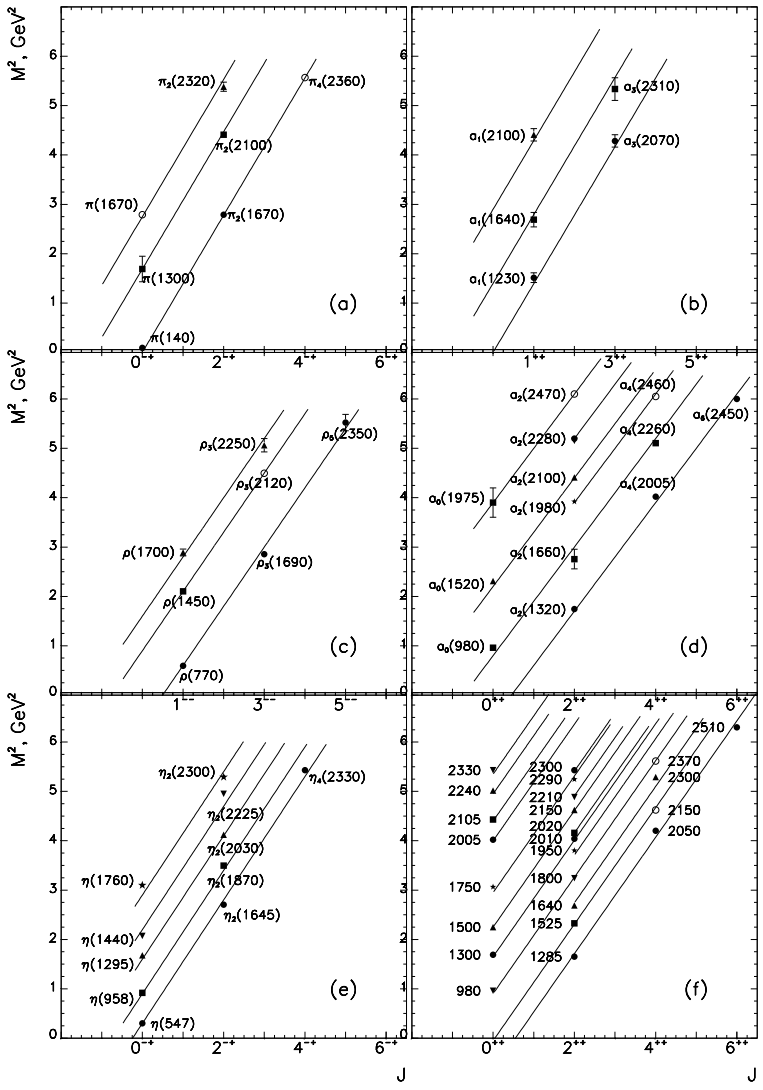

Figure 3: (J, M^2) planes for leading and daughter trajectories: a) π-trajectories, b) a_1-trajectories, c) ρ-trajectories, d) a_2-trajectories, e) η-trajectories, f) P'-trajectories.

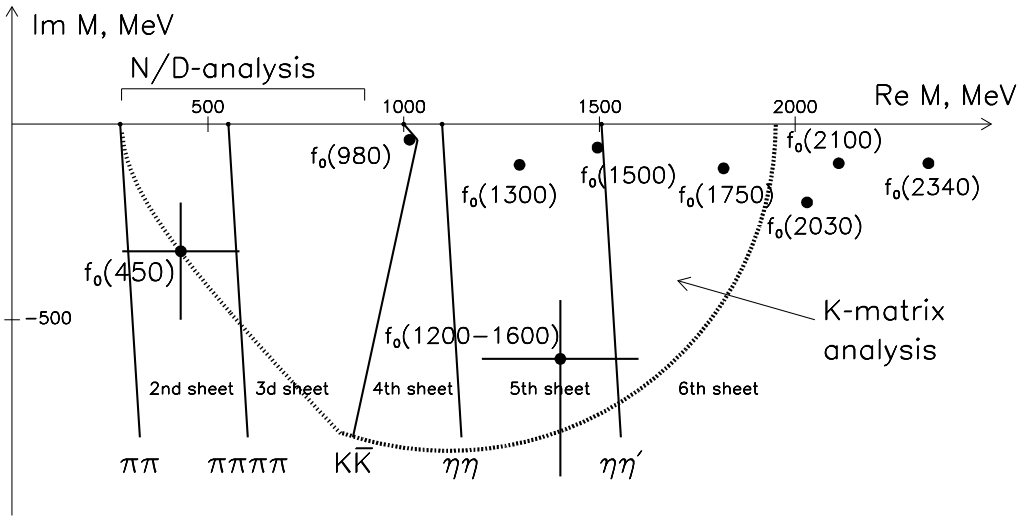

Figure 4: Complex M plane in the ($IJ^{PC} = 00^{++}$) sector. Dashed line encircle the part of the plane where the K-matrix analysis [8] reconstructs the analytic K-matrix amplitude: in this area the poles corresponding to resonances $f_0(980)$, $f_0(1300)$, $f_0(1500)$, $f_0(1750)$ and the broad state $f_0(1200-1600)$ are located. On the border of this area the light σ-meson denoted as $f_0(450)$ is shown (the position of pole corresponds to that found in the N/D method [31]). Beyond the K-matrix analysis area, there are resonances $f_0(2030), f_0(2100), f_0(2340)$ [6].

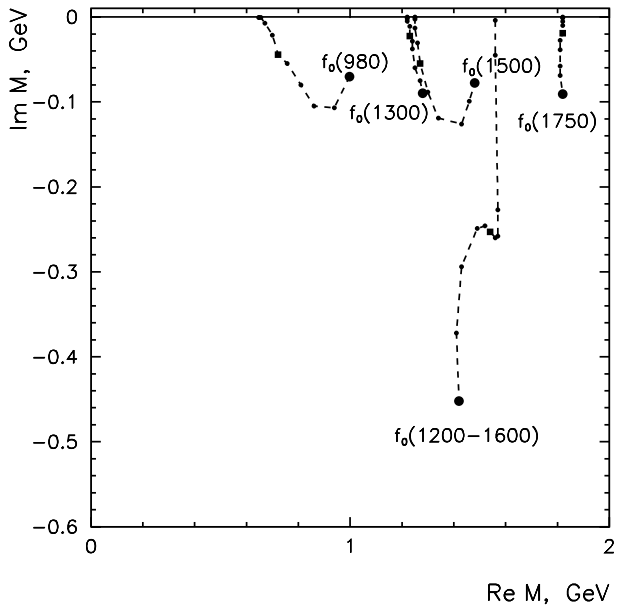

Figure 5: Complex M plane: trajectories of poles corresponding to the states $f_0(980)$, $f_0(1300)$, $f_0(1500)$, $f_0(1750)$, $f_0(1200-1600)$ within a uniform onset of the decay channels.

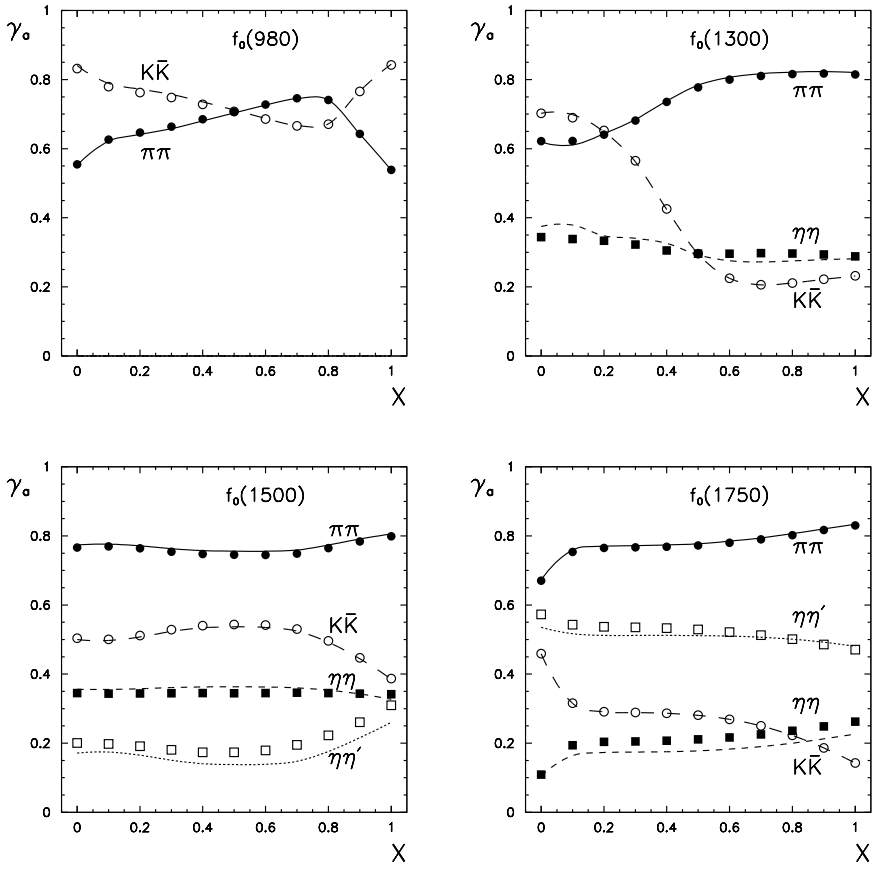

Figure 6: The evolution of normalized coupling constants $\gamma_a = g_a/\sqrt{\sum_b g_b^2}$ at the onset of the decay channels for $f_0(980)$, $f_0(1300)$, $f_0(1500)$, $f_0(1750)$. Curves demonstrate the description of constants by formula (38).

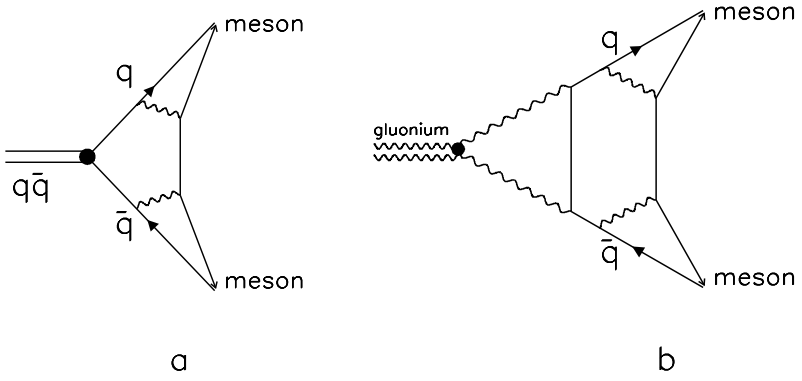

Figure 7: (a,b) Examples of planar diagrams responsible for the decay of the $q\bar{q}$-state and gluonium into two $q\bar{q}$-mesons (leading terms in the $1/N$ expansion).

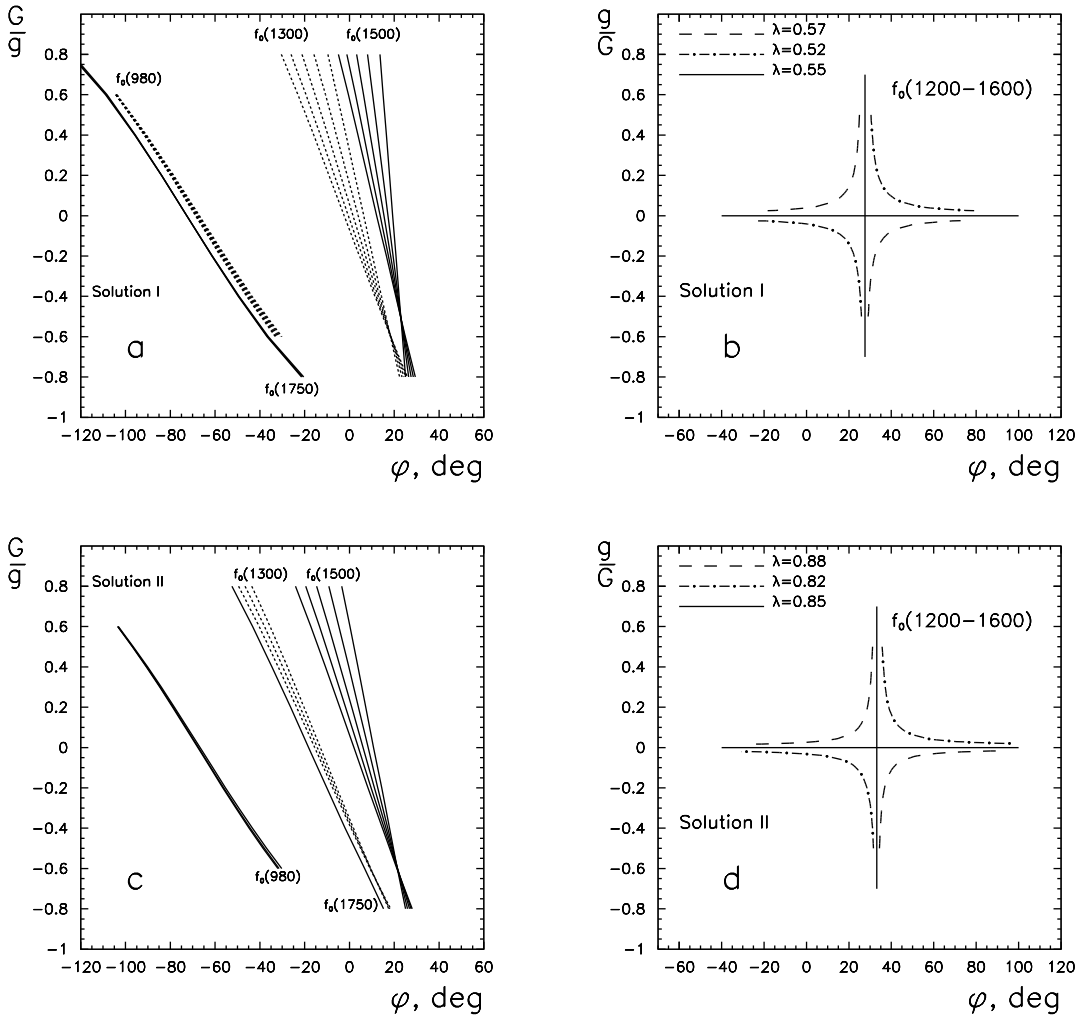

Figure 8: Correlation curves on the $(\varphi, G/g)$ and $(\varphi, g/G)$ plots for the description of the decay couplings of resonances (Table 4) in terms of quark-combinatorics relations (38). a,c) Correlation curves for the $q\bar{q}$-originated resonances: the curves with appropriate λ's cover strips on the $(\varphi, G/g)$ plane. b,d) Correlation curves for the glueball descendant: the curves at appropriate λ's form a cross on the $(\varphi, g/G)$ plane with the center near $\varphi \sim 30^\circ$, $g/G \sim 0$.

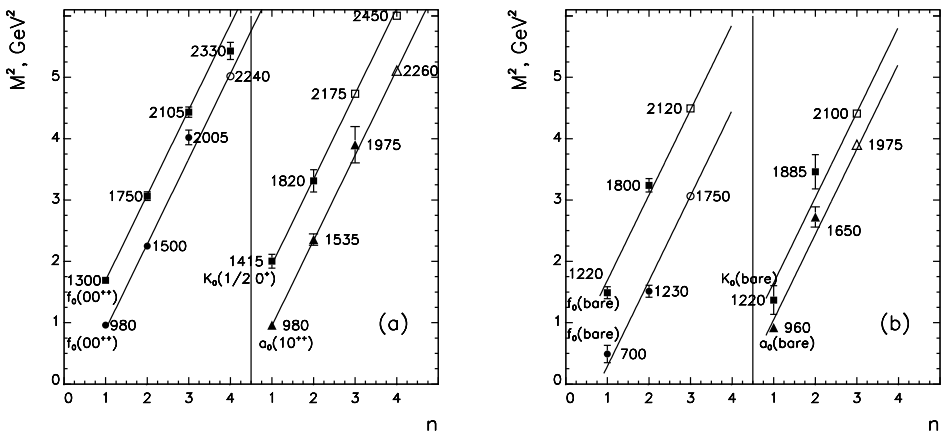

Figure 9: Linear trajectorieson the (n, M^2) plane for scalar resonances (a) and bare scalar states (b). Open circles correspond to the predicted states.

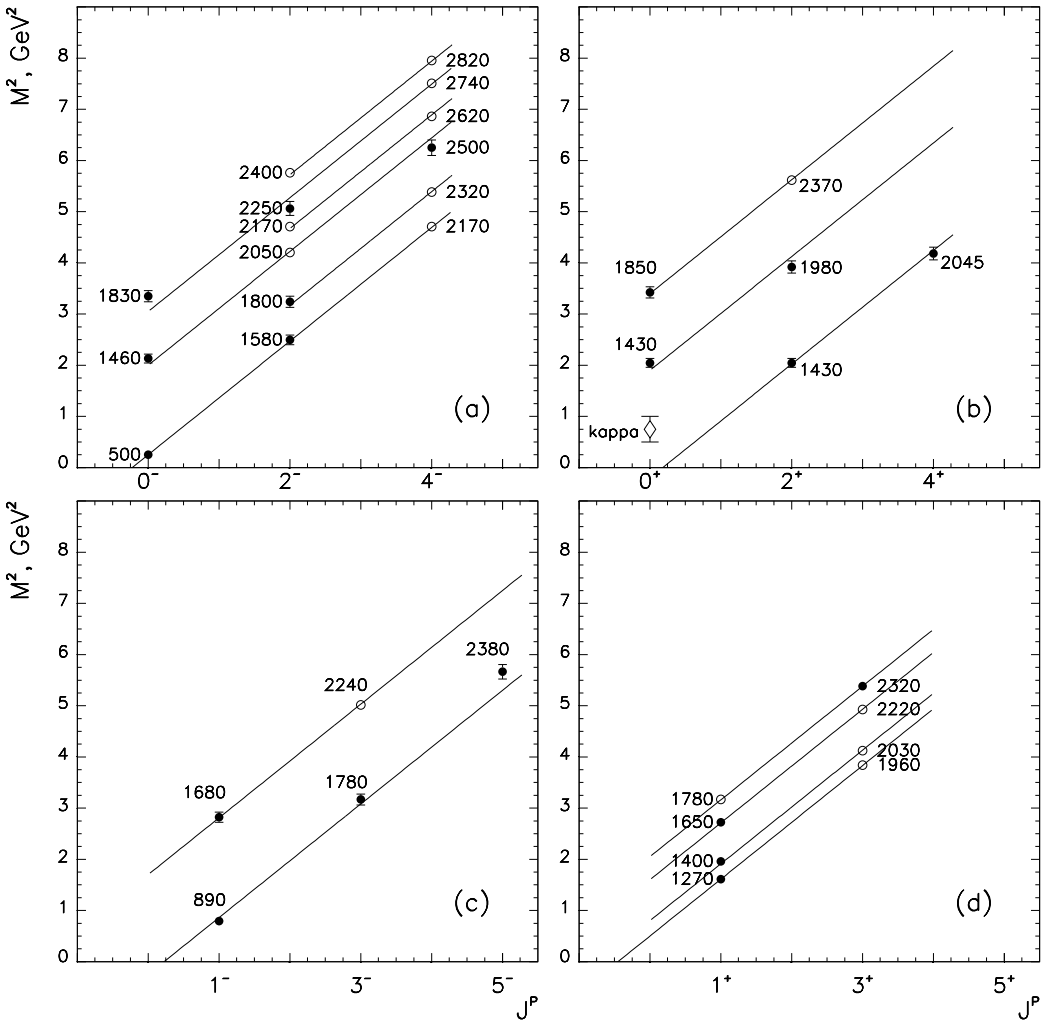

Figure 10: The (J^P, M^2) planes for kaonic sector (open circles stand for the predicted states).

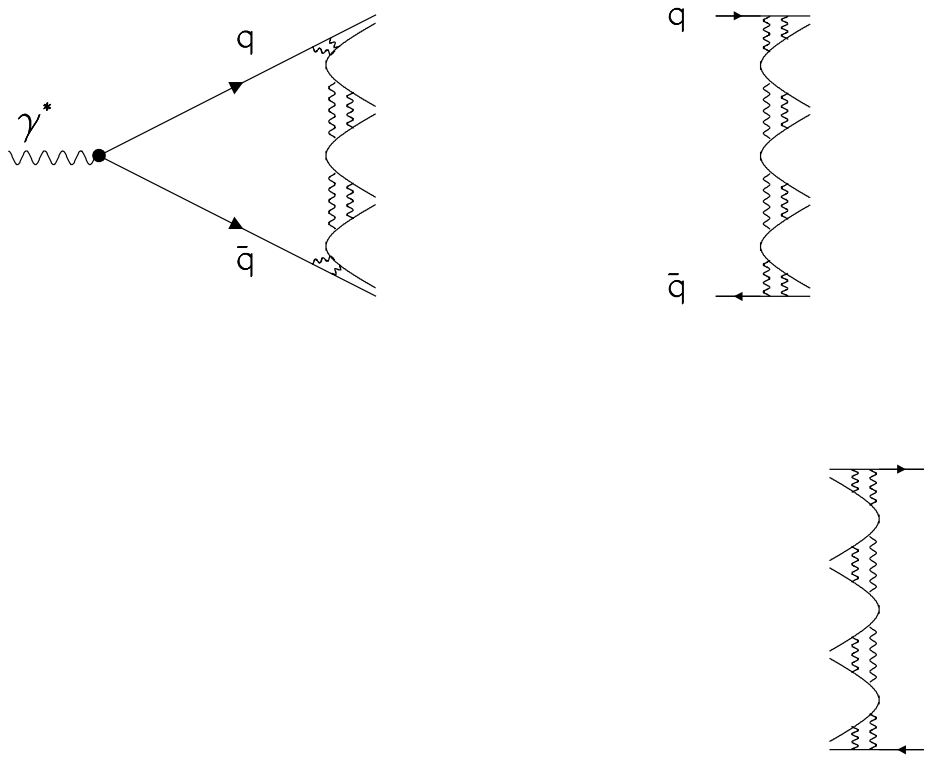

Figure 11: a) Quark-gluonic comb produced by breaking a string by quarks flowing out in the process $e^+e^- \to \gamma^* \to q\bar{q} \to mesons$. b) Convolution of the quark-gluonic combs — an example of diagrams describing interaction forces in the $q\bar{q}$ systems at $r \sim 2.0$ fm.